People's Democratic Republic of Algeria
Ministry of Higher Education and Scientific Research

Echahid Hamma Lakhdar University of El-Oued

FACULTY OF TECHNOLOGY

DEPARTMENT OF PETROCHEMICAL ENGINEERING

Master Thesis
Presented for graduation
ACADEMIC MASTER

Domain: Science and Technology

Sector: Petrochemical Industries

Speciality:Petrochemical Engineering

Theme

Production of Biodiesel Fuel From Food Waste

Presented by:

The jury composed of: - Chikha Belgacem Raihane

President: Oucif Khaled Mohammed Tayeb -ABDREBBI Abdallah

Examiner: Boughezal AbdeSlam - GHRISSI Nouh

Supervisor: Ahmouda Kouthar

2023/2024

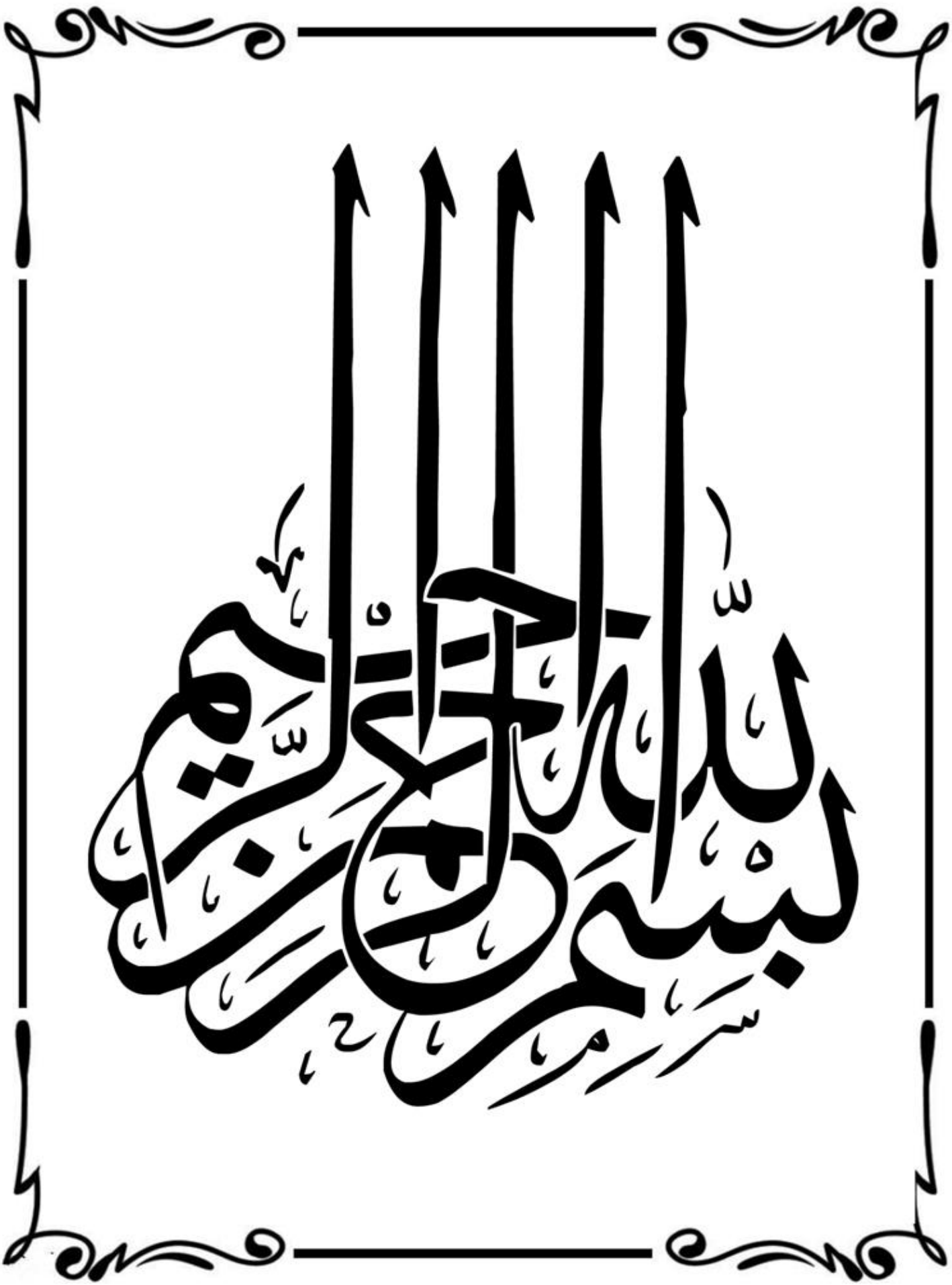
بسم الله الرحمن الرحيم

Thanks and Appreciation"

In the name of Allah, the Most Gracious, the Most Merciful

Praise be to Allah, through whose blessings good deeds are accomplished. Peace and blessings be upon the noblest of prophets and messengers, our Prophet Muhammad, and upon his family and companions.

We would like to extend our sincere thanks and appreciation to everyone who supported and stood by us throughout the journey of preparing this thesis. In particular, we would like to thank:

* -Our supervisor, Ahmouda Kaouthar, for her insightful guidance and valuable advice, which were fundamental in completing this work.

The esteemed faculty members, * especially the Dean of the College of Technology, Mr. Shamsa Ali, who provided invaluable assistance and guidance. We also extend our deep gratitude to the Dean of the College of Biology, Mr. Zaater Adelmalek, for his warm reception and for granting us access to his laboratories

We would also like to extend our gratitude to Mr. Oucif Khaled Mohammed Tayeb for welcoming us to the unit's laboratory.

Our beloved families, who provided us with moral and financial support and endured with us through periods of stress and pressure.

Our friends and colleagues, who were a source of support and assistance, whether through advice or practical help.

Without your support and encouragement, we would not have been able to reach this moment and successfully complete this thesis.

Abstract

This work investigates the production of biodiesel by ethylic esterification of cooking oil using five different catalysis which are: ARM-Fe_3O_4, ROS-Fe_3O_4, MAT-Fe_3O_4, JUN-Fe_3O_4 NPs, and KOH which is typically used as a basic catalyst. This work aims to study the impact of these different catalysts on produced biodiesel via their effect on the concentration of glycerol which is a by-product. The experiments were conducted under optimal conditions previously studied such as ration oil/ethanol (v%/v%), temperature and time of reaction, and the quantity of used catalysis. The findings showed that the use of MAT-Fe_3O_4, ARM-Fe_3O_4, and ROS-Fe_3O_4NPs as catalysts in biodiesel production leads to highly minimize the concentration of by-product glycerol where calculated concentrations are found to be:337.5 mM ,590 mM, and 592 mM, respectively. While that found by using JUN-Fe_3O_4 NPsand KOH are respectively 715Mm and 712 mM. So, MAT-Fe_3O_4, ARM-Fe_3O_4, and ROS-Fe_3O_4 NPs are more effective herein than KOH. Furthermore, the density (0.85 g/cm^3-0.87 g/cm^3) and kinematic viscosity (1.98CST -3.12CST) of produced biodiesel are found to be in international standards. The calculated yields of produced biodiesel are found to be 91%, 85%, 84%, 81%, and 82 %, respectively with catalysis of MAT-Fe_3O_4, ARM-Fe_3O_4, ROS-Fe_3O_4, JUN-Fe_3O_4 NPs, and KOH in biodiesel production. So, the use of MAT-Fe_3O_4, ARM-Fe_3O_4, ROS-Fe_3O_4 NPs as catalysts in biodiesel production is highly minimize the concentration ofby-product glycerol which in turn enhances the yield and the quality of biodiesel.

Keywords: Iron oxide nanoparticles,Biodiesel, Glycerol, Esterification, Catalyst

الملخص:

يحقق هذا العمل إنتاج الديزل الحيوي عبرالأسترة الإيثيلية لزيت الطهي باستخدام خمسة محفزات مختلفة هي: ARM-Fe_3O_4،ROS-Fe_3O_4،MAT-Fe_3O_4 NPs،JUN-Fe_3O_4،وKOH. يهدف هذا العمل إلى دراسة تأثيرهذه المحفزات المختلفة على الديزل الحيوي المنتج من خلال تأثيرها على تركيز الجليسيرول الذي يعد منتجًا ثانويًا. تم إجراء التجارب تحت ظروف مثلى تمت دراستها سابقًا مثل نسبة الزيت/الإيثانول (V%/V%)،درجة الحرارة و وقت التفاعل،وكمية المحفزالمستخدم. أظهرت النتائج أن استخدام محفزات أكسيد الحديد النانوية ARM-Fe_3O_4،ROS-Fe_3O_4،وMAT-Fe_3O_4في إنتاج الديزل الحيوي يؤدي إلى تقليل تركيزالجليسيرل بشكل كبير (590mM ، 592 mM،و337 mM على التوالي) مقارنة بتلك التي تم إنتاجها باستخدام JUN-Fe_3O_4 NPsوKOHوالتي كانت على التوالي 715 mM و712 mM. علاوة على ذلك،كانت كثافة (0.85-0.87) واللزوجة الكينماتيكية (1.9CST-12.CST)للديزل الحيوي ضمن المعاييرالدولية. وقد وجدت نسبة العوائد المحسوبة للديزل الحيوي المنتج 85%، 84%، 91%، 81%،و82% على التوالي بالنسبة للمحفزات النانوية المستخدمةARM-Fe_3O_4،ROS-Fe_3O_4،MAT-Fe_3O_4،JUN-Fe_3O_4،وKOH. لذا،فإن استخدام محفزات اكاسيد الحديد النانوية ARM-Fe_3O_4،ROS-Fe_3O_4،وMAT-Fe_3O_4في إنتاج الديزل الحيوي يؤدي إلى تقليل تركيز الجليسيرول المنتج الثانوي وبالتالي زيادة العائد وجودة الديزل الحيوي.

الكلمات المفتاحية: اكاسيد الحديد النانوية، البيوديزل ,الجليسيرول,المحفزات, الأسترة

Summary

Summary

CHAPTER II: IRON OXIDE NANOPARTICLES

List of Figures

List of Figures

List of tables

List of tables

GENERALE INTRODUCTION

General introduction

The global energy crisis and increasing environmental challenges are among the most critical issues facing the world today. Biofuels, particularly biodiesel, offer promising solutions to reduce reliance on fossil fuels and lower harmful emissions. Biodiesel is an alternative fuel produced from natural sources such as vegetable oils and animal fats through a process known as transesterification.

Catalysts such as basic ones KOH and NaOH play a crucial role in enhancing the efficiency of the biodiesel production process. This study examines the effectiveness of iron oxide nanoparticles as catalysts in increasing biodiesel yield and improving its quality., and comparing them with activity of KOH. Selecting the appropriate catalyst is essential for achieving high yield and excellent quality of the produced biodiesel.

One of the significant factors affecting biodiesel quality is the concentration of by-product glycerol produced during the production process. Excessive glycerol can negatively impact the properties of biodiesel, reducing its efficiency as a fuel. Therefore, minimizing glycerol content is crucial to ensure biodiesel meets high standards and complies with international requirements.

The importance of this study lies in providing practical solutions for improving biodiesel production using effective catalysts. The expected outcomes can enhance industrial biodiesel production processes, making them more efficient and yielding higher quality biodiesel, thereby making it more competitive as an alternative fuel. Additionally, this study can help reduce the environmental impact of conventional fuels, supporting global efforts to combat climate change.

This thesis is divided into three chapters:

1. **Chapter I: Overview of Biodiesel and Glycerol**
2. **Chapter II: Iron Oxide Nanoparticles**
3. **Chapter III: Production of biodiesel using different IONPs as catalysts**

Through this study, we aim to determine which type of iron oxide NPs is most effective in reducing the concentration of by-product glycerol and hence yield and quality of produced biodiesel.

Chapter I: Overview of Biodiesel and Glycerol

I.1 Introduction

Energy is a basic requirement for economic development for all nation. All sectors of the economy, including agriculture and industry transportation, commercial and household need energy. According to the advertised web article by US Energy Information Administration (EIA), energy consumption total global output was 406 quadrillion British thermal units (Btu) in 2000, and it is expected to rise to 769.8 quadrillion Btu by 2035, an increase of approximately 47.25%. Energy consumption will certainly increase further [1]. Energy demand development is the root of environmental problems and gas emissions global warming is one of the main reasons for fuel development alternatives of agricultural origin (biofuels) [2].

I-2- Biofuels:

The phrase "biofuel" (from the Greek pios, life, and the Latin carbo, coal, carbon) means that this fuel is obtained from organic materials. We also use the expression "green fuel". It might be better to call it “agrofuels.” Biofuels (or agrofuels) are fuels produced from renewable, non-fossil organic materials. They can be manufactured from oil, alcohol obtained by alcoholic fermentation of hydrolyzed sugars or starches, gaseous fuels obtained from plant or animal biomass (dihydrogen or methane), or coal [2].

I-3- Uses of vegetable oils as biofuels:

Up to 100% vegetable oil can be used as a biofuel for all diesel engines, subject to minor modifications to heat the fuel in question, or, without modification, blended with regular diesel (30% in all vehicles, up to 50% depending on the case) [2]. The main disadvantages of using vegetable oils and animal fats as biofuels are mainly related to their high viscosity (about 11 - 17 times higher than that of diesel fuel), and low volatility leads to the formation of deposits in engines due to incomplete combustion and incorrect evaporation properties. . These problems are associated with fatty chains of triglycerides with high molecular weights. These disadvantages can be circumvented: the triglycerides that make up vegetable oils can be converted into alcohol and glycerol esters by esterification reaction with methanol or ethanol. The smaller biodiesel particles thus obtained have properties similar to those of diesel fuel and can then be used as fuel in compression ignition engines. This biodiesel fuel contains no Sulphur, is non-toxic and biodegradable. Today it is often called Dyster (a marketing brand) [3].

I-4- Use of alcohols as biofuels:

I.4.1- Bioethanol:

It is produced by fermenting simple sugars from plants (beets, sugarcane) or starches from grains (wheat, corn) by yeast. It can be mixed directly with gasoline in proportions ranging from 5 to 26%, in equal proportions and in higher proportions for so-called “flexible” compounds. A small percentage of ethanol added to diesel can also be used but this practice is uncommon. In Europe, ethanol is most often incorporated into gasoline after it is converted to ETBE (ethyl tert-butyl ether) [4].

I-4-2 Ethyl tert-butyl ether (ETBE):

It is a derivative of ethanol. It is obtained by the reaction between ethanol and isobutene and is used as a 15% gasoline additive. Isobutene is obtained during petroleum refining. The ETBE/gasoline mixture has a lower vapor pressure than the ethanol/gasoline mixture and

therefore meets gasoline specifications. ETBE incorporation has the following advantages: no volatility problem, high octane number increase, and ideal water tolerance.

I-4- 3- Biobutanol (or butyl alcohol):

Obtained enzymatically from 1-butanol sugars (acetonobutyl fermentation). The driving idea behind using biobutanol as an alternative to gasoline is to take advantage of its physical advantages to circumvent the difficulties associated with the use of ethanol (volatility and aggressiveness towards some plastics used in the automotive industry). Biobutanol can be used as a fuel blended with gasoline up to 10% by volume without engine modification. It can also be used in mixtures with ethanol, gasoline or even diesel [4]. Bioethanol production units can be adapted to produce biobutanol.

I-4-4- Methanol (or "wood alcohol"):

It is obtained from methane and can also be used as a partial replacement (under certain conditions) for gasoline as an additive in diesel, or, in the long term, for certain types of fuel. fuel cells. But methanol is very toxic to humans.

I-4-5- Cellulosic ethanol:

The production of cellulosic ethanol involves fermentation. This route is implemented in 3 main stages. Of the three main components of lignocellulosic biomass (cellulose, hemicellulose and lignin) today only cellulose can be converted to ethanol. The first step is therefore to extract the cellulose and then convert it into glucose by hydrolysis using enzymes (enzymes produced in reactors from microorganisms (eg the fungus tricchodermareesei) are able to naturally hydrolyze cellulose into glucose). The glucose is then fermented by yeast and converted into ethanol. Finally, ethanol is purified by distillation and dehydration [5].

I-5- Microalgae:

This is an agricultural fuel made from microalgae or algae. Microalgae can provide different types of renewable energy. These include methane from anaerobic digestion of algae [6], biodiesel derived from microalgae oil [7, 8] as well as hydrogen production via photobiology [9, 10]. The idea of using microalgae as fuel sources is not new [11,12] but is starting to be taken seriously into consideration due to escalating oil prices and global warming associated with fossil fuel consumption [13].

I-6- Use biodiesel as fuel:

Biodiesel, a fatty ester of light alcohol, currently has many applications (diesel fuel, domestic fuel oils, environmental solvents, basic compounds for the manufacture of fatty alcohol sulfonates, amides, diesters, etc.) thanks to its chemical and physical structure. Properties very close to petroleum.

I-6-1-Oils: different sources, selection criteria, composition and properties:

I-6-1-1- Sources of different oils:

In principle, any fat source can be used to prepare biodiesel. However, some sources are preferred more than others depending on the country. Thus, in the United States, manufacturers use soybean oil. They are the largest producers of soybean oil before Brazil. On the other hand, Brazilians use different sources of oil due to the country's biodiversity. For example, in the north of the country mainly palm and soybean oil are produced, while in the Midwest soybean,

cottonseed, castor and sunflower oil are produced. In France, producers mainly use rapeseed oil [14].

I-6-1-2-Criteria for selecting vegetable oils as a source in biodiesel production:

The source (vegetable oil) of biodiesel must meet two very important criteria as much as possible: low production price, and large production scale. Edible oil prices, such as soybean oil for example, are higher than diesel prices. For this reason, it is preferable to use waste vegetable oils and non-edible vegetable oils as a source of fatty materials for the production of biodiesel. We can also use frying oils, peeling oils, various animal oils, such as fish oils, and even fats, because for the esters formed from these oils, we can get more than 10°C in temperature [15].

On the other hand, to choose a biodiesel source, it is important to take into account the percentage of oil in the plant and the oil yield per hectare. Take the United States, where replacing transportation diesel with biodiesel requires 0.53 billion cubic meters of biodiesel per year depending on the speed of current consumption. The table below shows the oil yields per hectare for different oil sources, the acreage required, and the percentage of area under cultivation in the United States. Thus, to produce 50% of the transportation fuels in the United States, it is necessary to devote 24% of the country's arable surface area to growing palm oil (the oil that is considered the most profitable). It is clear that vegetable oil will not be able to significantly replace petroleum derivatives in the future. However, this scenario changes dramatically when microalgae are used as sources. In fact, the required surface area is reduced by up to 1 to 3% [16].

I-6-1-3- Chemical and physical properties of vegetable oils:

The physical properties of biofuels are essential to influence the physical and chemical properties of the oil used for it: such as viscosity, melting point and thermal stability. Vegetable oils consist mainly of triglycerides, free fatty acids and by-products that are mainly: phospholipids (lecithin, cephalin) the source of mucilage, carotenoids and xanthophylls (polyunsaturated) which are highly polymerizable, tocopherols (natural antioxidants), and free sterols or esterification, triterpene alcohols, monoglycerides (which may crystallize), diglycerides, traces of water, silica, etc.

In some cases, poor artisanal oil production or insufficient storage can lead to a significant presence of these by-products [17].

Free acids, resulting from the hydrolysis of triglycerides, can be present at different levels, depending on the nature and method of storage of the oil. It can range from less than 0.5% for edible oils to 60% or more for highly acidic oils. Triglycerides are long molecules whose hydrolysis results in the formation of glycerol and three fatty acids. The general structure of triglycerides is as follows:

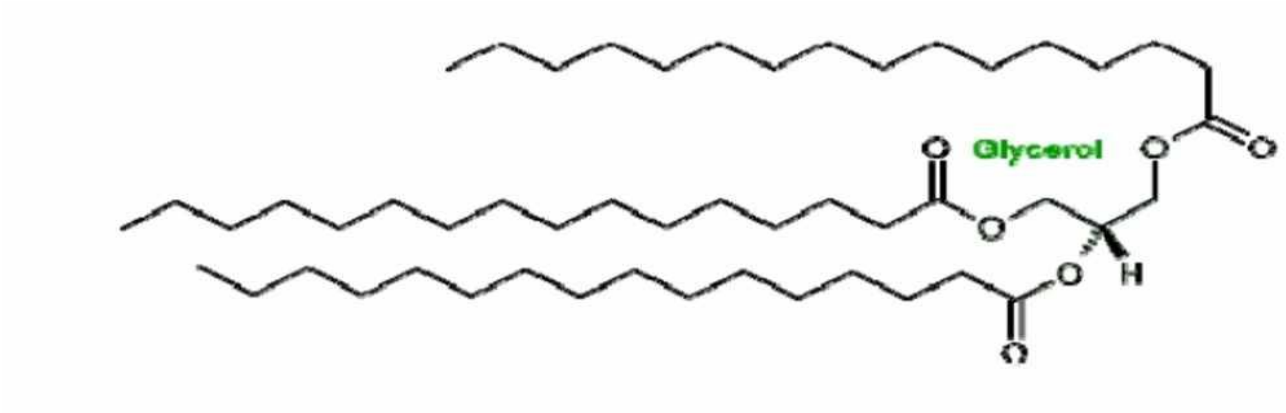

Figure I-1: General chemical structure of triglycerides

Fatty acids are classified into three categories: major, minor and unusual. We first mention the main fatty acids, which are the most widespread and in large quantities in plants, such as: lauric (C12), myristic (C14), palmitic (C16), stearic (C18), and oleic acid (C18:1). Linoleic (C18:2) and linolenic (C18:3). Secondly, secondary fatty acids, which are secondary components of fatty materials. Finally, unsaturated fatty acids are polyunsaturated fatty acids with conjugated or negligible double bonds, such as acetylene fatty acids (with triple bonds) or even fatty acids with a secondary function.

Triglycerides differ in their chain length, degree of unsaturation, and the presence of other chemical functions. They can be saturated, monounsaturated, or polyunsaturated. These double bonds that lead to unsaturation are found in chains containing more than 14 carbon atoms, and are not found at the end of the chain. They are fragile and easily oxidized to form peroxides and then carboxylic acids. For this reason, the oil should always be stored away from light, heat, and moisture. The effect of chain length takes precedence over the degree of unsaturation.

Oils have important basic chemical properties: iodine II, acidity indicators; AI and saponification; IS, cetane number, flash point and cloud point [18].

I-6-1-3-2- Chemical properties:

I-6-3-2-1- Iodine II index:

The iodine index is defined by measuring the mass of iodine (I2) (expressed in grams) that is able to bind to the known unsaturation double bonds of the fatty chains of 100 grams of fat. It is used to measure the amount of unsaturation. Oil with a high iodine content is not very resistant to oxidation, which can cause combustion problems (cracking and polymerization in the engine's combustion chambers). The oil is saturated and resistant to oxidation but is often solid at room temperature.

I-6-3-2-2- AI acidity index:

The acidity index is a measure of the mass of potash (expressed in mg) needed to neutralize the free fatty acids present in 1 gram of fat. This indicator is determined when cold, as it gives an idea about the thermal stability of the oil, especially the smoke point and flash point, which decrease sharply when the acidity of the oil increases. This can also lead to corrosion problems.

I-6-3-2-3-Saponification index:

The saponification index determines the mass of KOH in the mg needed to saponify the combined fatty acids in one gram of fatty substance. The saponification index is therefore an indirect measure of the PM molar mass of the fatty acids and hence the oil [18].

I-6-3-2-4-Cetane number:

The cetane number is used to evaluate the autoignition ability of diesel fuel on a scale from 0 to 100 [19]. This index appears to increase with the molecular weight of the fatty acid as well as with the molecular weight of the alcohol for the same fatty acid, while it decreases with the number of unsaturation [20,21]. In Europe, the lowest cetane index for diesel fuel is around 45; The average in France is close to 50.

I-6-1-4- Physical properties:

I-6-1-4-1- Density:

The density of vegetable oils is greater than that of diesel (about 10%). But this has little effect on the behavior of the motor or burner. However, the fuel flowmust be adjusted taking into account this difference in density and the fact that it varies with temperature [22].

I-6-1-4-2. Viscosity:

Viscosity depends largely on the nature of the fluid and its temperature. Vegetable oils and diesel behave like Newtonian fluids. Its viscosity evolves as a function of temperature according to the power law [23].

Viscosity affects the operation of a biodiesel engine or burner, including injection, atomization, vaporization and combustion. The high viscosity of the fuel, as is the case with vegetable oils (10 to 15 times higher than that of biodiesel), causes large pressure losses in the injection pump as well as in the filters, injectors or nozzle. In addition, we often encounter lubrication problems in some injection pumps at low temperatures, resulting in significant mechanical losses. The higher viscosity of vegetable oils is due to their higher molar mass (at least three times higher) compared to that of biodiesel[24].

I-6-1-4-3-Intake and flow points:

These two properties mainly determine the cold behavior of the fuel [25]. Cloud point (or Cloud Point, in English) is the temperature at which a product cooled under uniform conditions begins to show crystals. Its value determines the tendency of the product to clog the filters [26].

As for the pour point (or pour point), it represents the lowest temperature at which the cooled product under uniform conditions is likely to continue to flow. It specifies the conditions for storing, transporting and “pumping” fuel. The more saturated the vegetable oil, the greater these two properties. This is the case for some saturated oils (palm, coconut), which are solid at room temperature (generally). In contrast, unsaturated oils such as rapeseed and cottonseed oils have relatively low draw and flow points [26].

I.-7- Waste cooking oils used as a source of biodiesel:

I-7-.1 Oils used and the environment:

The feed cutter is a product of detergents, especially used food oils. Valorizing these oils used in biodiesel production prevents aberrations in the killing process and thus protects water production facilities and the environment.

I-7-2 Chemical composition of furnace oils:

In the presence of water, oxygen, and high temperatures between 160°C and 180°C, triglycerides are exposed to a large number of unwanted reactions and complexes. They can be classified into three large families: oxidation, polymerization, and hydrolysis [27].

I-7-2-1 Oxidation reactions:

Compounds form	Origin	Type of alteration
•Oxidized monomers •Dimers •Volatile compounds	Air oxygen	Oxidation
•Cyclicmonomers •Non-polar dimers	Bath temperature	Thermal
•Free fatty acids •Diglycerides	Food water	Hydrolysis

Table I.1:Main pathways for the formation of new chemical species

Cooking oils coming into contact at high temperatures with oxygen in the air causes unwanted odor and discoloration.

These unwanted redox compounds are derived from hydrogen peroxides, which are primary compounds of redox. Reactions in the chains responsible for their formation are stimulated spontaneously, by the appearance of radical compounds, giving rise to a simulation of triglyceride oxidation. Metal cations such as iron or metal can initiate and accelerate oxidation reactions [28].

I-7-2-2 Polymerization reactions:

They are responsible for the inter- and intramolecular rearrangements that sense the friction oil oxidation and help increase the apparent viscosity of the oils [29].

I-7-2-3 Hydrolysis reactions:

They are more numerous under normal friction conditions. Contact with water vapor leads to the formation of mono- and diglycerides: leads to the formation of glycerol. The presence of caustic cleaning product residues favors hydrolysis reactions [30].

I-8-Biodiesel synthesis method:

I-8.-1- Pyrolysis:

Pyrolysis is the decomposition of an organic product to produce others, only under the effect of heat, or accompanied by the use of a catalyst. It is possible to perform pyrolysis of vegetable oils, animal fat, natural fatty acids and fatty acid methyl esters. The chemistry of pyrolysis is difficult to interpret given the number of chemical pathways the reaction can encounter, as well as the variety of products that can be obtained. The thermal decomposition of these structures occurs via the formation of free radicals or by carbonium ions. Testing of pyrolyzed oils on engines is limited in the short term [31].

I-8-2-dilution:

Diluting vegetable oil is another method of using it as a fuel [3]. The dilution of sunflower oil with diesel in a ratio of 1:3 by volume was studied and tested by Ziejewski et al [32]. The viscosity of this mixture was 4.88 cSt at 40°C. They concluded that this mixture cannot be recommended for long-term use.

1-8-3-Transesterification:

Transesterfication or alcoholysis is the reaction between an ester and an alcohol giving an ester with properties different from those of the oil [33].

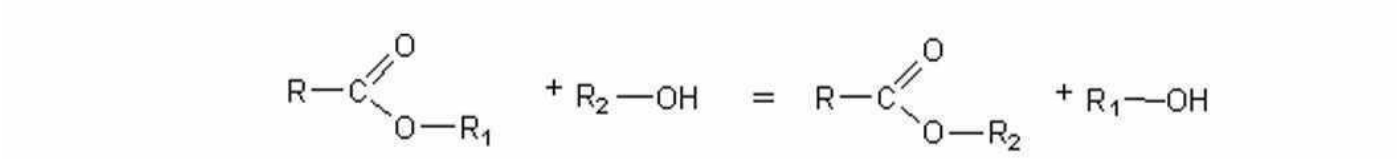

Figure I-2:General reaction of transesterification

It involves the reaction between the triglyceride contained in a vegetable oil with an alcohol to form glycerol and a mixture of monoesters used as biofuel [29].

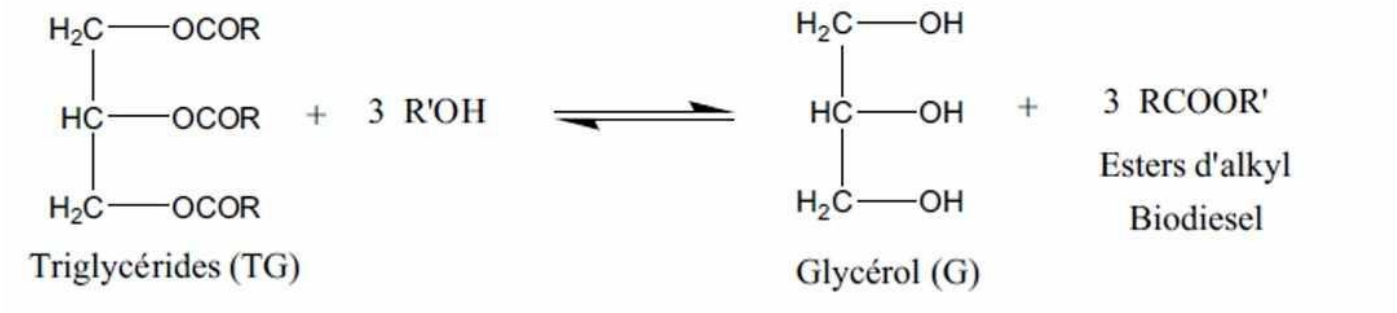

Figure I-3: Transesterification reaction of triglycerides with alcohol

The transesterication of alcoholic oils is catalyzed by acids or bases. It is favored by an increase in temperature, an excess of alcohol, the type of catalyst used, or when the operating conditions allow the decantation of the glycerol [33].

I-9-Main homogeneous and heterogeneous catalysis:

I-9-1-homogeneous catalysis:

Catalysis is said to be homogeneous when the catalyst and reactants form only one (often liquid) phase. It is the most widely used catalysis and can be performed using basic or acidic catalysts.Homogeneous catalysis requires moderate temperature and pressure: 45 to 85°C under a maximum absolute pressure of 2.5 bars [34].

I-9-1-1-Basic homogeneous catalysis:

Basic catalysts are used due to their high reactivity and non-corrosive nature.Sodium hydroxide (NaOH) and potassium hydroxide (KOH) are the most widely used basic catalysts for various reasons such as: their ability to catalyze at low temperature and atmospheric pressure, the importance of the conversion rate achieved in the shortest possible time, their widespread availability and little use price[35].

I-9-1-2- Acidic homogeneous catalysis:

The catalysts often used are mineral acids such as hydrochloric acid, H_2SO_4, H_3PO_4, and sulfonic acids such as paratoluenesulfonic acid [36].Acid catalysis makes it possible to overcome parasitic reactions that can damage the reaction product because they are insensitive to essential fatty acids and can simultaneously catalyze the reaction of essential fatty amino acid esterification and triglyceride transesterification.

It has been reported in the literature that the acid catalyst becomes more effective when the FFA content in the oil exceeds 1% by mass. However, it has also been shown that the transesterification process under acid catalysis is much slower than the process under basic catalysis. Friedman et al. [37] showed that under acid catalysis, the transesterification process is 4000 times slower.Thus, due to the low reactivity and very slow kinetics, acid catalysis requires stringent conditions during the transesterification reaction, such as for example: high reaction temperature, high alcohol/oil molar ratio, and large reaction time. In addition, due to the corrosive nature of acid catalysts, maintenance of industrial plants becomes difficult and expensive [36].

I-9-2- Heterogeneous catalysis:

It is a catalytic process in which the catalyst and reactants form several phases (generally solid catalyst to solid or liquid phase reactants). It requires extreme temperature and pressure conditions (180°C to 200°C, 40 to 60 bars). Therefore, it is not suitable for laboratory conditions and small and medium enterprises[34].

I-9-2-1-Heterogeneous acid catalysis:

Solid acid catalysts can easily replace liquid acid catalysts. The advantages of using solid acid catalysts are numerous: their ability to convert triglycerides and transesterify free acids in order to increase yields, eliminate the biodiesel washing step, and easily separate the catalyst in the reaction medium, ensuring minimal contamination of the medium. product and finally, regenerate and reuse the catalyst while reducing the corrosion problem, even in the presence of acidic species [36].

I-9-2-2- Basic heterogeneous catalysis:

The basic heterogeneous catalysts used in the biodiesel industry are classified according to their importance, such as alkaline earth oxides, mixed metal oxides, alkali metal salts on porous supports, zeolites or even solid organic bases. Basic solid catalysts in biodiesel production have been developed, such as basic zeolite, alkali oxides, alkali earths, and hydrotalcite. Among these catalysts, oxides have attracted attention due to their relatively high basicity, low solubility in alcohol and the possibility of being produced from less expensive raw materials [38].

I.10 Glycerol definition:

Glycerol, also known as glycerin or glycerine, is a simple polyol compound with the chemical formula $C_3H_8O_3$. It is a colorless, odorless, and viscous liquid that is sweet-tasting and non-toxic. Glycerol is a trihydroxy alcohol, meaning it has three hydroxyl (OH) groups, which contribute to its high solubility in water. This compound is a central component of triglycerides, which are the main constituents of body fat in humans and animals, as well as vegetable oil. In the industrial context, glycerol is a by-product of soap and biodiesel production, obtained from the saponification or transesterification processes.

Due to its unique chemical properties, glycerol has a wide range of applications in various industries. In the pharmaceutical and personal care industries, glycerol is used as a humectant, solvent, and sweetener. It is a key ingredient in many skincare products, such as lotions and creams, due to its moisturizing properties. Additionally, glycerol is utilized in the food industry as a sweetener, preservative, and thickening agent. Its ability to retain moisture makes it valuable in extending the shelf life of food products. Furthermore, glycerol is employed in the production of antifreeze, plastics, and as a raw material for the synthesis of other chemicals.

I-10-1 Glycerol is indesirable by- product

In the context of biodiesel production, glycerol is a significant by-product. The transesterification process, which converts fats and oils into biodiesel, produces glycerol in a ratio of approximately 10% of the total product. Managing this by-product is crucial, as the accumulation of glycerol can affect the efficiency and economics of biodiesel production. Researchers are exploring various ways to utilize and add value to crude glycerol, such as converting it into value-added chemicals, using it as a feedstock for microbial fermentation, or refining it for use in pharmaceutical and food industries. Efficiently managing glycerol by-product not only enhances the sustainability of biodiesel production but also opens up new avenues for its application.

I-10-2 Thechnics used to minimise glycerol production:

Minimizing the production of glycerol during biodiesel production is crucial for enhancing the efficiency and economic viability of the process. Here are some methods used to achieve this:

I-10-2-1Optimizing Reaction Conditions:

Optimizing the reaction conditions such as temperature, time, and molar ratio of alcohol to oil can significantly influence the amount of glycerol produced during biodiesel synthesis. Typically, lower reaction temperatures and shorter reaction times can help minimize glycerol

formation. Additionally, fine-tuning the molar ratio of alcohol to oil ensures complete transesterification with minimal by-product generation.

I-10-2-2Using Alternative Catalysts:

The choice of catalyst plays a vital role in the biodiesel production process. Traditional catalysts such as sodium hydroxide (NaOH) or potassium hydroxide (KOH) can lead to significant glycerol by-product. Using alternative catalysts like heterogeneous catalysts (e.g., metal oxides, ion-exchange resins) or enzyme-based catalysts (lipases) can reduce glycerol production. Heterogeneous catalysts, in particular, can be easily separated from the reaction mixture and reused, reducing the formation of side products.

I-10-2-3Implementing Glycerol Removal Techniques:

In-situ glycerol removal techniques involve the continuous extraction of glycerol from the reaction mixture during the transesterification process. This can be achieved through techniques like membrane separation, where a selective membrane allows the passage of biodiesel while retaining glycerol. Another approach is to use a decanter or centrifuge to separate glycerol from biodiesel in real-time. By continuously removing glycerol, the equilibrium shifts towards increased biodiesel production and reduced glycerol formation.

I-10-2-4Co-solvent Method:

The co-solvent method involves adding a co-solvent such as tetrahydrofuran (THF) or acetone to the reaction mixture. The co-solvent helps in dissolving both oil and methanol, creating a homogeneous phase that facilitates the reaction and reduces the formation of glycerol. This method can enhance the reaction rate and yield of biodiesel while minimizing the glycerol by-product.

I-10-2-5Using Advanced Nanocatalysts:

The use of nanocatalysts, such as iron oxide nanoparticles (Fe3O4 NPs), has shown promise in reducing glycerol production. These catalysts provide a high surface area for the reaction to occur, enhancing the reaction rate and selectivity towards biodiesel production. Nanocatalysts can also be engineered to have specific properties that minimize side reactions leading to glycerol formation.

By employing these methods, biodiesel production can be made more efficient with a lower glycerol by-product, enhancing the overall economic and environmental sustainability of the process.

Conclusion:

Biodiesel production is a sustainable alternative to traditional fossil fuels, offering environmental and economic benefits. However, the process often results in the formation of glycerol as a by-product, which can affect the quality and yield of the biodiesel. Minimizing glycerol production is essential to enhance the efficiency of biodiesel synthesis, ensuring that the final product meets international standards for density and kinematic viscosity. By optimizing reaction conditions, using alternative catalysts, and employing advanced techniques such as nanocatalysts and supercritical fluid technology, the production of glycerol can be significantly reduced. This not only improves the overall yield and quality of biodiesel but also supports its viability as a competitive and eco-friendly fuel source.

Chapter II :
Iron Oxides NPs

II-1- Introduction:

Iron and its compounds have been used in various industries and applications throughout the ages, but the use of nano-iron or nanoparticles in modern technology is considered more recent. Research in the field of nanotechnology and nanomaterial manufacturing has provided a better understanding of the properties and potential applications of these materials.

For example, in recent years, scientists and engineers have begun to use nanotechnology to design and develop specific iron nanoparticles to achieve new properties and innovative applications. Historically, innovative research and applications of nanoscale iron oxides have been documented in scientific literature and technical reports in recent years, where they are used in areas such as renewable energy, medicine, materials performance enhancing technologies, and many other applications.

With the development of technology and continued research in the field of nanotechnology, it is expected that nanoscale iron oxides will continue to be a topic of interest and research in the coming years, opening the way for more cutting-edge innovations and applications.

II-2- Definition of nanosized iron oxides:

Nanoscale iron oxides are iron particles whose dimensions typically range from 1 to 100 nanometers. These molecules are used in a variety of technical and scientific applications due to their unique properties, such as their high energy storage potential and thermal and electrical conductivity. Nanoscale iron oxides have a large surface area compared to their small size, which enhances their chemical reactions and their ability to interact with other materials efficiently. They are used in applications such as biotechnology, renewable energy, and performance improvement technologies in many industrial and research fields.

II-3-Types of nanoscale iron oxides:

There are several types of nanoscale iron oxides, which differ in their chemical composition, properties and applications. The most famous of these types are[40]:

II-3-1- Iron Oxide Nanite (Fe_2O_3):

Also known as red iron oxide or hematite. It has its distinctive red color and is used in applications such as medical imaging, pharmaceuticals and energy storage.

II-3-2- Iron(II) oxide (Fe_3O_4):

also known as magnetite. It has strong magnetic properties, making it useful in magnetic applications such as data storage and medical diagnosis.

II-3-3-Iron (III) oxide (FeO):

This type is black in color and is used in catalase and electrochemical storage applications.

II-3-4- Properties of iron oxide nanoparticles:

Nanoscale iron oxides have several distinct properties due to their small size and structural composition. Here are some of its main characteristics:

II-3-5-Small particle size:

Iron oxide nanoparticles typically range in size from 1 to 100 nanometers, giving them a large surface area relative to their size, which enhances their chemical reactivity and physical properties[41].

II-3-6-Magnetic properties:

Some types of nanoscale iron oxides such as Fe_3O_4 (magnetite) exhibit strong magnetic properties, making them useful in magnetic storage and medical diagnostic applications.

II-3-7-Energy storage potential:

Some nanoscale iron oxides exhibit high energy storage properties, making them candidates for use in energy storage applications such as batteries and fuel cells.

II-3-8-Electrical and thermal properties:

Nanoscale iron oxides may exhibit unique electrical and thermal properties, which can be exploited in applications such as thin electronic devices and thermal insulation materials.

II-3-9-Catalytic activity:

Some nanoscale iron oxides exhibit catalytic activity, making them useful for catalase applications in areas such as energy conversion and chemical process optimization [42].

II-3-10-Enhanced surface response:

Due to their large surface area compared to particle size, nanosized iron oxides can exhibit enhanced surface response, making them candidates for use in sensitive applications such as sensing and imaging technologies.

These are some of the main properties of nanoscale iron oxides, and the exact properties depend on the chemical composition and crystal structure of each type.

II-3-11- Green manufacturing of iron oxide nanoparticles

Green manufacturing technology aims to reduce the environmental impact of manufacturing processes and use natural and sustainable materials in industrial processes. Green manufacturing principles can be applied to the manufacture of iron oxide nanoparticles in several ways, including[43]:

II-3-12-Use of environmentally friendly raw materials:

Using natural and renewable raw materials such as plant compounds or other organic materials in preparing solutions or gases used in preparation processes[44].

II-3-13-Using renewable energy:

Employing renewable energy sources such as solar energy or biothermal energy to operate Reducing waste and emissions: Applying pollution control methods, reducing waste and harmful emissions during manufacturing processes, and treating waste in an environmentally friendly manner.

II-3-14-Using efficiency improvement technologies:

Using advanced and innovative technologies to improve the efficiency of manufacturing processes and reduce the consumption of natural resources and energy.

II-3-15-Controlling environmental risks:

Providing the necessary measures to reduce the potential environmental risks of the chemicals used and prevent their leakage into the environment.

Applying green manufacturing principles in the fabrication of nanoscale iron oxides can contribute to reducing the negative environmental impacts of industrial processes and enhancing sustainability in the chemical and technological industry.manufacturing equipment and heating processes.

II-4- Areas of use of nano-iron oxides:

Nanoscale iron oxides are used in a wide range of fields due to their distinctive properties and multiple applications, including:

II-4-1-Renewable energy technology:

Nanoscale iron oxides are used in renewable energy storage systems such as solar batteries and fuel cells, where they can improve energy conversion efficiency and increase storage capacity.

II-4-2-Biomedical technologies:

Nanoscale iron oxides are used in medical diagnostic applications such as magnetic resonance imaging (MRI) and targeted drug delivery, where they can improve diagnostic accuracy and reduce side effects.

II-4-3-Nanoelectronics and devices:

Nanoscale iron oxides are used in nanoelectronics applications such as tablets and storage devices, where they can improve device performance and increase energy efficiency.

II-4-4-Smart Materials and Smart Coatings:

Nanoscale iron oxides can be used to manufacture smart materials and smart coatings that respond to ambient conditions such as temperature and humidity, and are used in applications such as thermal insulation and anti-corrosion coatings.

II-4-5-Environmental and purification applications:

Nanoscale iron oxides are used to purify and desalinate water, and remove environmental pollutants such as mercury and contaminated organic materials, as they can improve water quality and reduce pollution.

II-4-6-Insulation and thermal insulation applications:

Nanoscale iron oxides can be used in thermal insulation and sound insulation applications in buildings and structures, as they can effectively reduce heat and sound transmission.

These are some of the main areas of use of nanoscale iron oxides, and there are more potential applications in various industries and research fields[45].

II-5-The role of nanosized iron oxides as catalysts:

Nanoscale iron oxides are effective catalysts in many chemical reactions and biological processes due to their unique nano-level properties. Here are some of the major roles of nanoscale iron oxides as catalysts:

II-5-1-Catalyzing chemical reactions:

Nanoscale iron oxides are used as catalysts in a number of chemical reactions, such as the conversion of hydrocarbons, redox reactions, and thermal decomposition reactions, as they can speed up these processes and increase their efficiency.

II-5-2-Reduced activation energy:

Nanoscale iron oxides contribute to reducing the activation energy required .

II-5-3-Increased active zone surface:

Thanks to their small size and nanostructure, nanosized iron oxides have a relatively large surface compared to their size, which means increased active zone surface available for reaction.

II-5-4.-Selective response

Nanoscale iron oxides allow a more selective response to certain compounds or reactions making them ideal catalysts for specific reactions.

II-5-5-For use in bioanalysis and diagnostics:

Nanoscale iron oxides can be used in bioanalytical and medical diagnostic applications, such as improving the response of immunological tests and increasing diagnostic sensitivity.

II-5-6-Transportation and storage technologies:

Nanoscale iron oxides are used in transportation and storage technology applications such as improving the magnetic properties of materials and developing magnetic storage technologies.

Overall, it can be said that nanoscale iron oxides play an important role as catalysts in a wide range of industrial and scientific applications, contributing to improving process efficiency and reducing costs and the environment[46].

Conclusion:

Iron oxide nanoparticles (IONPs) have emerged as highly effective catalysts in various chemical processes, including biodiesel production. Their unique properties, such as high surface area, magnetic characteristics, and catalytic efficiency, make them particularly suitable for enhancing reaction rates and selectivity. In biodiesel production, IONPs facilitate the transesterification process, leading to higher yields and better quality of the final product.

The advantages of using IONPs as catalysts include their ability to operate under milder conditions, reducing the energy input and minimizing the need for harsh chemicals. Additionally, their magnetic properties allow for easy separation and reuse, promoting a more sustainable and cost-effective production process. The application of IONPs in biodiesel production not only improves the efficiency and yield but also contributes to environmental sustainability by providing a cleaner alternative to conventional fossil fuels. As research progresses, the potential of iron oxide nanoparticles in various catalytic applications continues to expand, underscoring their significance in advancing industrial processes and promoting green chemistry.

Chapter III: Production of biodiesel by using different catalysts and control of glycerol concentration

III-1-Introduction:

In this practical section of the thesis, we will detail the steps and procedures followed to convert used cooking oil into biodiesel. This section aims to provide an accurate description of the experiments, equipment, and chemicals used in the process, as well as discuss and analyze the results. The chemical conversion of used cooking oil into biodiesel involves several key stages, including pre-treatment, the transesterification reaction using iron oxide nanoparticles which are among the most effective catalysts for biodiesel product, and the final purification of the product. The outcomes of each stage will be presented and the efficiency of the process in producing high-quality biodiesel will be evaluated. Through this work, we aim to demonstrate the effective potential of converting waste oil into clean and sustainable fuel, thereby contributing to reducing environmental impact and promoting the use of renewable resources.

III-2-Preparation of Plant Extract and Green Synthesis of Iron Oxide NPs

In this section, used methods for plant extract preparation and characterization, as well as the green synthesis of iron oxide NPs and characterization techniques are described as well .

III-2-1-Plant Extract Preparation

The preparation of the aqueous plant extract dealt with in this studywhich are:(Artemisia herba-alba Matricaria pubescens Juniperus Phoenicia Rosemarinus officinalis) is described here. Firstly, we well-washed the plant with doubly distilled water. After being dry, they are ground into fine powder. Afterward, 30g of fine powder plant is mixed with 540mL of doubly distilled water. To well extracting the antioxidant substances, the mixtures are stirred continually for 24h with a stirrer at ambient temperature. Next, the extract is passed through two layers of muslin and the liquid is then passed through 0.22 µ filters (Millipore) to be used in later the green synthesis reaction as a reducing agent[47].

III-2-2-Green Synthesis of Iron Oxide NPs

For the green synthesis of iron oxide NPs, the followed protocol wasused: 200 mL of plant aqueous extract:(Artemisia herba-alba Matricaria pubescens Juniperus Phoenicia Rosemarinus officinalis) is mixed with 100 mL of aqueous iron chloride salt solution with concentration 0.4 M. The mixtures are stirred continually for 1h at reaction temperature 70 °C. They are then dried in the drying oven (Figure III-1). They are next washed several times with deionized water. Finally, they are stored for four months under ambient conditions. The phases of the obtained product are identified by XRD in the 2θ range of 10 − 90°. FTIR-ATR provides additional confirmation on the presence of the oxide phase as well as information on the sample's crystallinity. The surface investigation is done with the scanning electron microscope (SEM). UV-Vis spectroscopy is a technique widely used to examine the optical properties such as the band gap energy of the synthesized products (Total Attenuated Reflectivity). All measurements are achieved at ambient conditions of temperature and pressure [47].

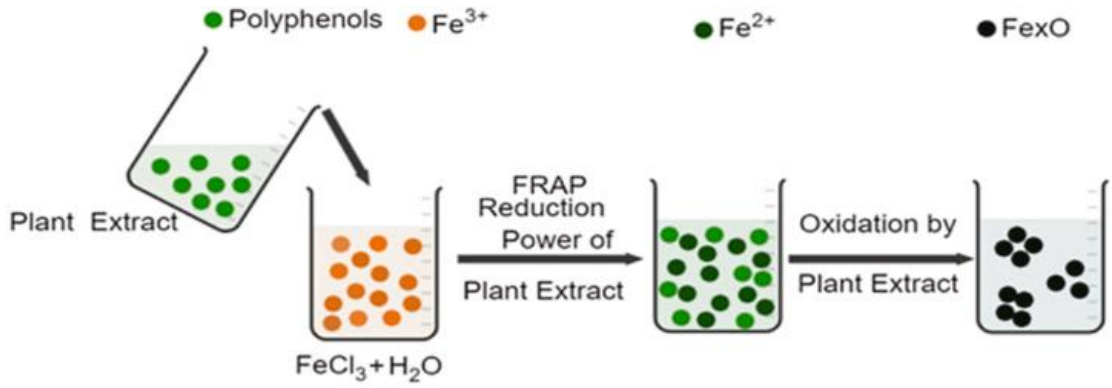

Figure III-1:protocol of green synthesis of iron oxide nanoparticles

III-3-Results and discussion:

The eco-friendly synthesis method of freshly prepared iron oxides NPs aswell as their characterization are thoroughly detailed in a previous work [40].In the eco-friendly synthesis of iron oxide NPs, the bioactive compoundsin mediating plant extract including polyphenols play a crucial role as are reducing agent. The overall reaction mechanism involving the reduction ofiron ions and the formation of iron oxide NPs can be described as follows:

• 1- Ferric ions ($\boldsymbol{Fe^{3+}}$are reduced to ferrous ions ($\boldsymbol{Fe^{2+}}$) by the bioactive compounds in the plant extract as presented in the next equation:

$$2\boldsymbol{Fe^{3+}} + \text{Polyphenols} \longrightarrow 3\boldsymbol{Fe^{2+}} + \text{Oxidized product} \quad (1)$$

• 2- Nucleation and formation of Iron(II) oxide NPs (FeO) as presented in the next equations:

$$n\boldsymbol{Fe^{2+}} \rightarrow \text{Nuclei} \quad (2)$$

$$\text{Nuclei} + \frac{\boldsymbol{1}}{\boldsymbol{2}}\boldsymbol{O_2} \rightarrow \boldsymbol{FeO} \quad (3)$$

3- In the presence of oxygen, the formed FeO NPs can undergo oxidation to produce $\boldsymbol{Fe_3O_4}$ NPs as presented in the next equation:

$$\boldsymbol{6FeO + O_2 \rightarrow 2Fe_3O_4} \quad (4)$$

Chen et al. reported that after four months of storage of FeO NPs underambient conditions, FeO NPs are completely oxidized to form a single phaseof $\boldsymbol{Fe_3O_4}$NPs. For this reason, after ending the synthesis, obtained ironoxide NPs($\boldsymbol{FeONPs + Fe_3O_4NPs}$) are stored for four months under theambient conditions to obtain one single phase of NPs which is$\boldsymbol{Fe_3O_4}$ NPs.

III-3-1-. X-ray Diffraction Analysis of Four Magnetite NPs:

The XRD patterns of the four iron oxide NPs samples are presented in(Figure III-2) and all exhibit Bragg reflection peaks at identical angles, howeverwith different peak intensities. These differences are mainly due to mediatingplant extract.

(Figure III-2)shows that peaks appear at around 2θ= 52.60◦, 49.80◦, 42.50◦,41.40◦, 41.00º,37.10º, 32.30◦, 30.80◦, 29.95◦, 25.60◦, 22.52◦, 20.30◦, 16.70◦,and 16.20◦. All of these peaks correspond to the $\boldsymbol{Fe_3O_4}$ phase and are consistent with the Miller indices 644, 534, 522, 251, 250, 404, 106, 106, 400,030, 212, 210, and 021, respectively, according to standard diffraction of orthorhombic$\boldsymbol{Fe_3O_4}$ NPs as defined in the JCPDF file 01-076-0958, except forminor differences

in intensities and a shift in 2θ◦ values arising from defectswithin magnetite NPs structures.The average diameters of the magnetite NPs samples, presented in (Table III-)1, were calculated using the next equation of Scherrer's:

D =0.9λ / β cos θ(5)

Where; θ, λ, and β represent the Bragg angle, the X-ray wavelength (1.54056˚A), and the full width at half-maximum (FWHM) of the most intense diffraction peak D represents the average diameter of the magnetite NPs.

The mostuseful information to be extracted from XRD patterns, in additionally to theaverage diameters, is the lattice parameters of$\boldsymbol{Fe_3O_4}$ FNPs samples. For orthorhombic crystal cells, lattice parameters are calculated using the followingequation[47]:

$$\frac{1}{d_{HKL}^2} = \frac{H^2}{a^2} + \frac{k^2}{b^2} + \frac{l^2}{c^2} (6)$$

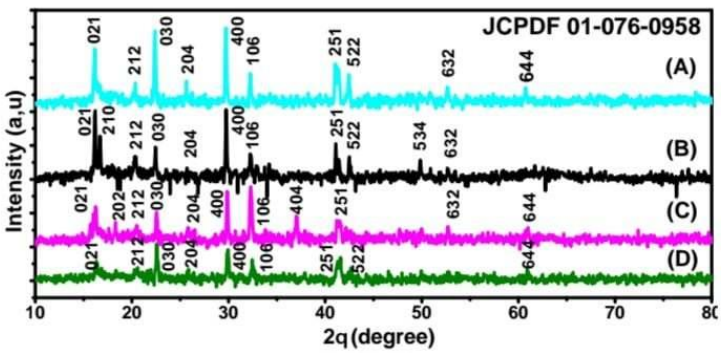

Figure III-2: XRD patterns of four magnetite NPs (A) ROS−$\boldsymbol{Fe_3O_4}$, (B) ARM−$\boldsymbol{Fe_3O_4}$(C) MAT−$\boldsymbol{Fe_3O_4}$, and (D) JUN−$\boldsymbol{Fe_3O_4}$, JCPDF file 01-076-0958,where, d_{hkl}, (hkl), and (a, b, c) are the inter-planer distance, Miller indices,and lattice parameters respectively

For $\boldsymbol{Fe_3O_4}$orthorhombic crystal cells,standard d_{hkl} = 2.96700˚A, and standard lattice parameters are a = 11.8680˚A,b = 11.8510˚A, and c = 16.7520˚A. The lattice parameters of the four orthorhombic magnetite NPs samples are calculated in the most intense diffraction peaks. a (˚A) is calculated with the help of peak 400, b (˚A) is calculatedwith the help of peak 030, and c (˚A) is calculated with the help of peak 021.

Magnetite NPs	Average Diameter (nm)	Calculated d ($\AA$)	Lattice parameters ($\AA$)
$ARM-Fe_3O_4$	41.49	2.97336	$a = 11.8934,\ b = 11.84151,\ c = 14.4107$
$ROS-Fe_3O_4$	39.89	2.97395	$a = 11.8958,\ b = 11.83656,\ c = 14.4466$
$MAT-Fe_3O_4$	33.13	2.97525	$a = 11.9010,\ b = 11.82426,\ c = 14.5370$
$JUN-Fe_3O_4$	29.27	2.97109	$a = 11.8844,\ b = 11.81994,\ c = 14.5690$

Table III-1: Crystallographic data obtained from XRD patterns of four magnetite NPs

When comparing the calculated lattice parameters presented in (TableIII-1) with the lattice parameters of the cell, minor differences are remarked dueto defects within magnetite NPs structures.

Furthermore, the results showed that the particle sizes of the magnetitesamples vary with the variation of the plant extract used in their eco-friendlysynthesis. The average diameter of the ARM−Fe_3O_4, ROS−Fe_3O_4, MAT−Fe_3O_4, and JUN −Fe_3O_4 NPs, presented in (TableIII-1), are, respectively, 41.49,39.89, 33.13, and 29.27nm.

It is well-known that the bioactive compounds including polyphenols andorganic acids in the plant extract, play a crucial role in stabilizing the formediron oxide nanoparticles (NPs). These compounds attach to the nanoparticlesurfaces, preventing agglomeration and ensuring stability, thereby reducingthe diameter of the particles. Mediating extracts' acidic pH of ARM−Fe_3O_4,ROS − Fe_3O_4, MAT − Fe_3O_4, and JUN − Fe_3O_4 NPs were, respectively,5.25, 5.05, 4.63, and 3.69. Consequently, the average diameter of Fe_3O_4NPs samples decreases with the increasing acidity of the plant extract. Thisfinding aligns with the results reported by Makarov et al. In their study, the authors environmentally prepared two samples of Fe_3O_4NPs using H.vulgare plant extract with a pH of 5.8 and R. acetosa plant extract with apH of 3.7. They observed thatFe_3O_4 NPs prepared using a less acidic plant extract exhibited smaller diameters.

III-3-2-FTIR-ATR Spectroscopic Analysis of Magnetite NPs:

FTIR spectroscopy is commonly used as an identification technique toobtain an idea about the phase of iron oxide NPs. Each iron oxide phaseproduces a distinguishable IR spectrum. The FTIR spectra of the four ironoxide NPs, which were recorded between 4000 and 500 cm^{-1}, are shown in FigureIII-3[40].

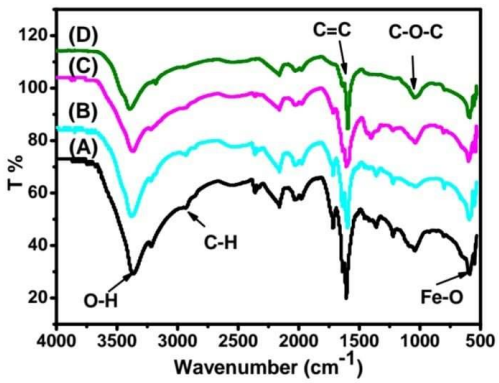

Figure III-3: FTIR spectra of eco-friendly prepared of (A) ARM−Fe_3O_4, (B) ROS−Fe_3O_4, (C) MAT−Fe_3O_4, and (D) JUN−Fe_3O_4 NPs

Table III-2: FTIR spectra of four magnetite NPs show varied vibration ranges of functionalgroups

Sample	$O-H$ cm^{-1}	$C-H$ cm^{-1}	$C=C$ cm^{-1}	$C-O-C$ cm^{-1}	$Fe-$ cm^{-}
$ARM-Fe_3O_4$	3267	2932	1590	1036	593
$ROS-Fe_3O_4$	3250	2930	1591	1039	592
$MAT-Fe_3O_4$	3236	2930	1591	1040	592
$JUN-Fe_3O_4$	3223	2929	1595	1039	594

Table III-2: summarizes the different peak ranges observed in the IR spectraof the four nanoparticle samples (Figure III-3 (A), (B), (C), and (D)). Peaks at 3223−3267$\boldsymbol{cm^{-1}}$ are attributed to O−H stretching vibration, while peaksat 2930−2932$\boldsymbol{cm^{-1}}$correspond to C−H aromatic and C−H aliphatic vibrations of $\boldsymbol{Fe_3O_4}$NPs. Peaks at 1590−1595$\boldsymbol{cm^{-1}}$correspond to C=C stretchin aromatic rings and anti-symmetric stretching of the carboxylate groups(COO−), whereas peaks at 1033−1045$\boldsymbol{cm^{-1}}$are assigned to the C−O−C ofthe phenolic groups. Additionally, the peak observed at around 590 $\boldsymbol{cm^{-1}}$is attributed to the F e−O stretching band of $\boldsymbol{Fe_3O_4}$NPs.

III-3-3-UV-Vis Spectroscopic Analysis of Four Magnetite NPs:

To determine the band gap energies of the four $\boldsymbol{Fe_3O_4}$ samples, theiroptical absorbance spectra were measured within the wavelength range of200−900 nm. The band gap (Eg) and the linear optical absorption coefficient (α) of a band gap semiconductor are connected through the followingequation:

$\alpha h\nu = A(\boldsymbol{h\nu - Eg})^{\boldsymbol{n}}$ (7)

In E_g, hν represents the energy of a photon, A is a constant of proportionality, and the value of the exponent n depends on the type of electronictransition that occurs; for indirectly allowed transitions, n = 2, while fordirect allowed transitions, n = 1/2.

The band gap energies of the four magnetite samples were determined using theextrapolation of the linear portion of the plot $(\alpha h\nu)^2$ vs αhν (Figure III-4) for direct transition E_g values, and the plot $(\alpha h\nu)^{1/2}$ vs αhν (FigureIII-5)for indirect transition E_g values.

The estimated direct and indirect band gap energies of the four magnetite samples are presented in (TableIII-3) [47].

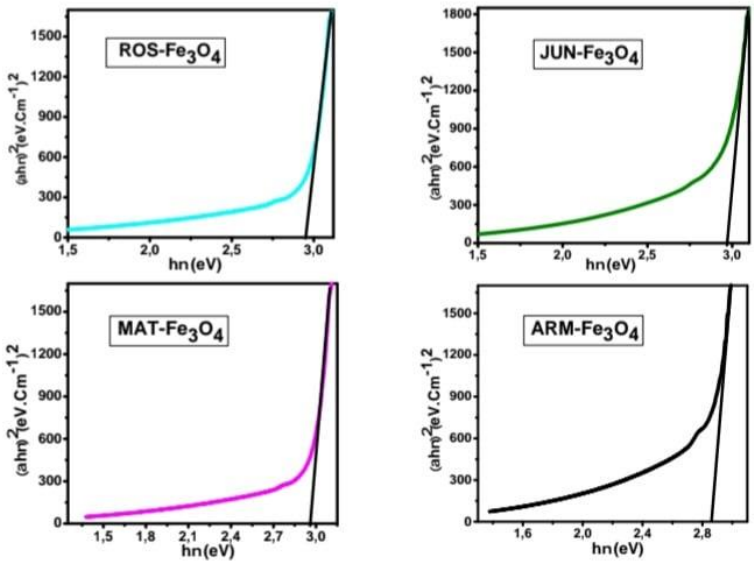

Figure III-4: Plots of $(\alpha h\nu)^2$ versus $(\alpha h\nu)$ for direct transition of four Fe_3O_4samples sonicated in acetone for 15 minutes

The direct band gap energy $E_g$values for ARM−Fe_3O_4, ROS−Fe_3O_4, MAT−Fe_3O_4, and JUN−$Fe_3O_4$are 2.87eV, 2.95eV, 2.96eV, and 2.97eV, respectively. These valuesare comparable to the result obtained by Kamakshi et al. where theyreported a direct band gap energy of 2.76 eV for magnetite NPs. Indirectband gap energy values were also estimated for the four samples using thesame method and are also shown in (Table III-3). The estimated indirect E_g values for ARM−Fe_3O_4, ROS−Fe_3O_4, MAT−Fe_3O_4, and JUN−Fe_3O_4samples were found to be 2.51, 2.55, 2.60, and 2.64eV, respectively, whichare comparable to the indirect E_g reported in reference (E_g = 2.53eV).

Table III-3: Estimated direct and indirect band gap energies of four magnetite NPs

Sample	direct E_g (eV)	indirect E_g (eV)
$ARM-Fe_3O_4$	2.87	2.51
$ROS-Fe_3O_4$	2.95	2.55
$MAT-Fe_3O_4$	2.96	2.60
$JUN-Fe_3O_4$	2.97	2.64

The estimated direct and indirect band gap energies of the four magnetitesamples fall within the range of band gap energies of semiconductors, whichtypically range from 0-3 eV [60].

Therefore, it is reasonable to classify thefour magnetite samples as semiconductors based on their band gap energies.

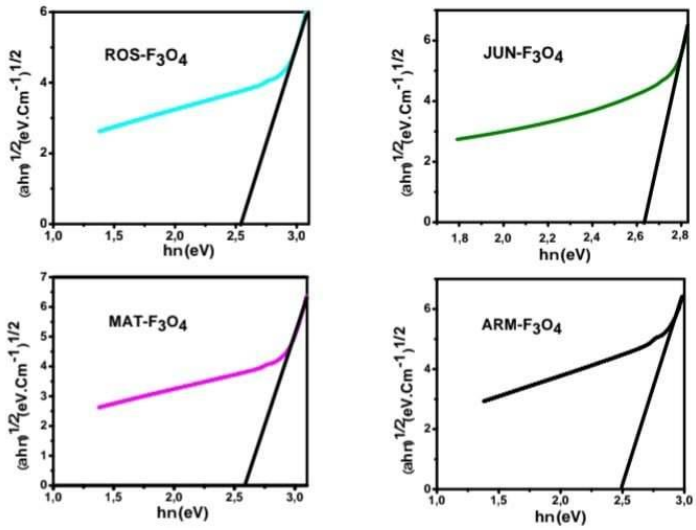

Figure III-5: Plots of $(\alpha h\nu)^{1/2}$ vs $(\alpha h\nu)$ for indirect transition of four Fe_3O_4NPs sonicatedfor 15 minutes in acetone

Furthermore, it is found that the diameter of ARM−$\boldsymbol{Fe_3O_4}$, ROS−$\boldsymbol{Fe_3O_4}$, MAT−$\boldsymbol{Fe_3O_4}$, and JUN−$\boldsymbol{Fe_3O_4}$ NPs is respectively, 41.49, 39.89, 33.13,and 29.27nm. the smaller crystallite size of eco-friendly prepared$\boldsymbol{Fe_3O_4}$NPsis related to the higher direct and indirect $\boldsymbol{E_g}$. values as proof of the quantumsize effect. So, the decrease in particle diameter leads to an increase in the$\boldsymbol{E_g}$. This result is in agreement with that reported by Singh et al [47].

III-3-4-SEM Images of Eco-friendly Synthesized Magnetite NPs:

(Figure III-6) depicts SEM images of the four magnetite samples synthesizedusing plant extract, revealing their irregular rock-like forms. Agglomeration assembling rocks are evident in the SEM image of JUN−$\boldsymbol{Fe_3O_4}$NPs (Figure III-6a), while MAT−$\boldsymbol{Fe_3O_4}$NPs exhibit mountain-like structures with giantrocks (FigureIII-6b). ROS−$\boldsymbol{Fe_3O_4}$and ARM−$\boldsymbol{Fe_3O_4}$SEM images displayoccasionally big structured single bipyramids crystals, as observed in (FiguresIII-6c and 6d)[40].

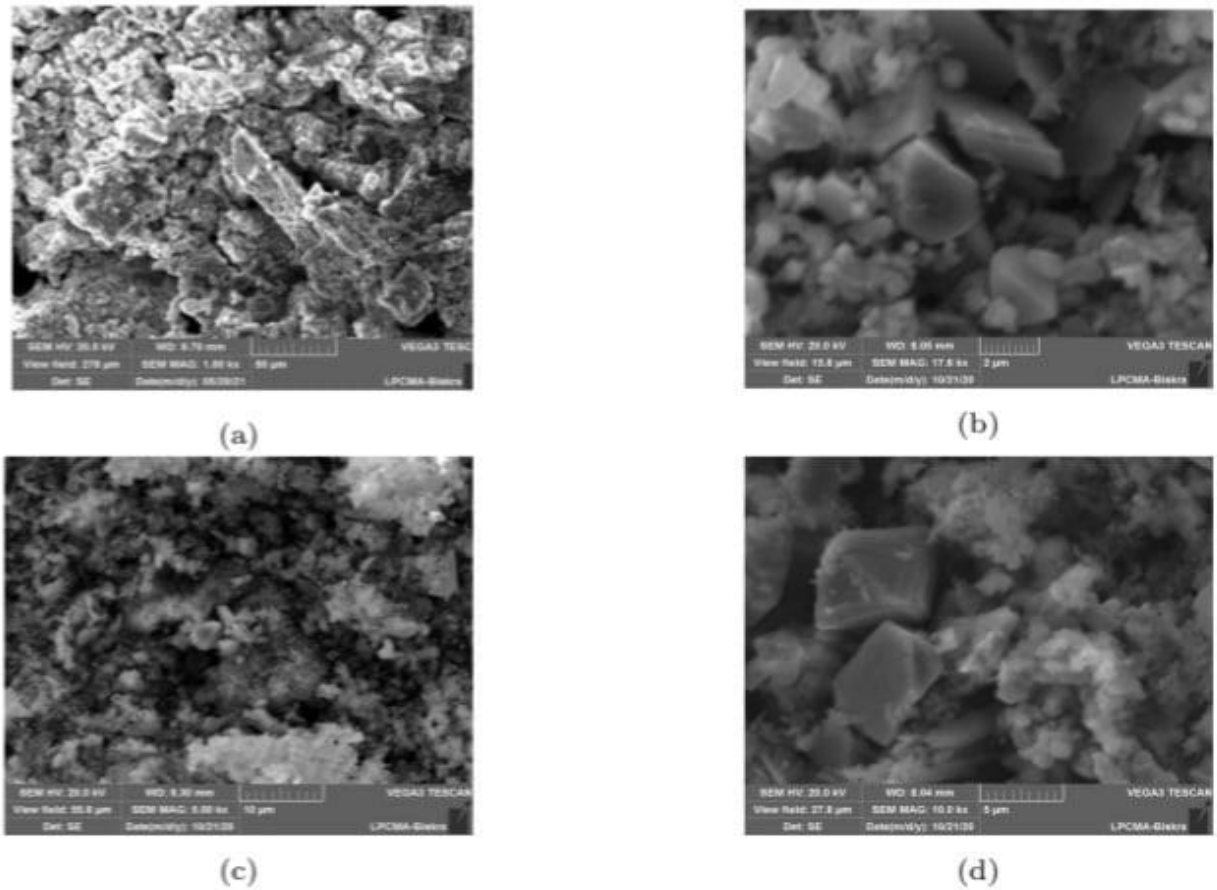

Figure III-6:SEM images of eco-friendly synthesized (a) JUN−Fe_3O_4 ,(b) MAT−Fe_3O_4NPs),(c) ROS−Fe_3O_4, and (d)ARM−Fe_3O_4

III-4-Protocol for the Synthesis of Biodiesel via Ethylic Transesterification Reaction of Used Sunflower Oil from Frying

In this section biodiesel was produced via ethylic esterification of cooking oil by using different IONPs and KOH as catalysts.

III-4-1-Chemicals and Apparatus

III-4-1-1-Chemicals:

Chemicals used in experiments are listed below.

- Used sunflower oil from frying, provided by our family kitchen;
- Ethanol (C_2H_5OH, 95%, SIGMA Aldrich);
- Potassium hydroxide (KOH, 98%, SIGMA Aldrich) as a homogeneous catalyst;
- Ironoxide NPs: **ARM** $-Fe_3O_4$,**JUN** $-Fe_3O_4$,$MAT-Fe_3O_4$, $andROS-Fe_3O_4$as heterogeneous catalysts;
- Glycerol($C_3H_8O_3$,98%, SIGMA Aldrich);
- Bi-distilled water.

III-4-1-2-Apparatus

Apparatus used in experiments are listed below.

- A balance;
- Hot plate;
- Thermometer;
- Magnetic stirrer;
- Condenser;
- Ultrasonic cleaner;
- Viscometer;
- Densimeter;
- Spectrophotometer;
- Centrifuge.

III-4-2-Experimental protocols:

III-4-2-1-Preparation of calibrate curve of glycerol:

To determine the concentration of glycerol produced in each biodiesel experiment, we prepared a calibration curve. Various concentrations of glycerol (ranging from 100 mM to 1000 mM) were prepared, and their absorbances were measured at the maximum absorbance wavelength (λ = 230 nm). By plotting the absorbance values against glycerol concentrations, we created a calibration curve. This curve will be used to determine the concentration of glycerol by-product produced during biodiesel production.

III-4-2-2-Production of biodiesel using different catalysis:

In order to determine which catalysts highly minimize glycerol concentrationduring the production of biodiesel, we conducted several catalysts$\mathbf{ARM}-\boldsymbol{Fe_3O_4}$,$\mathbf{JUN}-\boldsymbol{Fe_3O_4}$,$\boldsymbol{MAT}-\boldsymbol{Fe_3O_4}$,$\boldsymbol{ROS}-\boldsymbol{Fe_3O_4}$ and KOH were used.

The optimization of experimental conditions, including temperature, reaction time, oil/ethanol ratio (v/v), and catalyst mass, was previously studied by Ahmouda et al. (2019, Master's thesis). They determined that the optimal conditions were: an oil/ethanol ratio of 30%/70% (v/v), a reaction temperature of 65°C, a catalyst mass of 0.1 g, and a reaction time of 30 minutes. Therefore, these optimal conditions have been adopted in our experiments.

III-4-2-2-1- ARM $-Fe_3O_4$NPs Catalyst :

During conducting experiment of production of biodiesel by the use of **ARM** $-Fe_3O_4$ as catalysis, next steps are followed:

- Cooking oil was filtered by a (filter paper) multiple times to obtain clear oil.
- we dissolved 0.1g of **ARM** $-Fe_3O_4$ in 210ml of ethanol.
- We added the previous mixture to 90ml of cooking oil.
- The mixture is placed on an Ultrasonic for 30 minutes at a temperature 65°C.
- After the reaction, the mixture is transferred to a condenser to remove the ethanol to avoid moisture, and we take the mixture to the centrifuge to remove the catalyst from it, then we added hot water twice (85°C), each time using 25ml with stirring
- After completing the experiments, we placed the mixture (glycerol with biodiesel) in the separator for 24 hours to separate of organic (biodiesel) and aqueous phases (aqueous glycerol) .

Figure III-7: The mixture (glycerol with biodiesel) in the separator for 24 hours

III-4-2-2-2-$ROS-Fe_3O_4$NPs Catalyst :

During conducting experiment of production of biodiesel by the use of **ROS** $-Fe_3O_4$as catalysis, next steps are followed:

- Cooking oil was filtered by a (filter paper) multiple times to obtain clear oil.
- we dissolved 0.1g of $ROSFe_3O_4$in 210ml of ethanol.
- We add the previous mixture to 90ml of cooking oil.
- The mixture is placed on anUltrasonic for 30 minutes at a temperature of 65°C.
- After the reaction, the mixture is transferred to a condenser to remove the ethanol to avoid moisture, and we take the mixture to the centrifuge to remove the catalyst from it, then we add hot water twice (85°C), each time using 25ml with stirring.
- Separation of organic (biodiesel) and aqueous phases (aqueous glycerol) for 24 hours (Figure III-8-2).

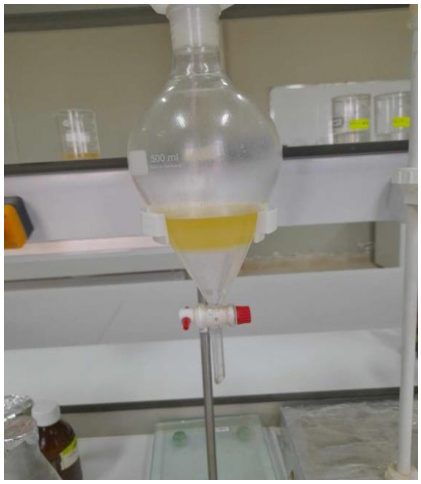

Figure III-8: The mixture (glycerol with biodiesel) in the separator for 24 hours

III4-2-2-3-JUN $-Fe_3O_4$ *NPs* catalyst :

During conducting experiment of production of biodiesel by the use of **JUN $-Fe_3O_4$**as catalysis, next steps are followed:

- We filtered the used cooking oil multiple times to obtain clear oil.
- we dissolved 0.1g of **JUN $-Fe_3O_4$**in 210ml of ethanol.
- We added the previous mixture to 90ml of cooking oil.
- The mixture is placed on anUltrasonic for 30 minutes at a temperature of 65°C.
- After the reaction, the mixture is transferred to a condenser to remove the ethanol to avoid moisture, and we take the mixture to centrifuge to remove the catalyst from itthen we added hot water twice (85 °C), each time using 25ml with stirring. (Figure III-8-3).
- Separation of organic (biodiesel) and aqueous phases (aqueous glycerol) for 24 hours (Figure III-8-3).

Figure III-9: The mixture (glycerol with biodiesel) in the separator for 24 hours

III-4-2-2-4-*MAT* $-Fe_3O_4$ *NPs* catalyst :

During conducting experiment of production of biodiesel by the use of **JUN $-Fe_3O_4$**as catalysis, next steps are followed:

- We filtered the used cooking oil multiple times to obtain clear oil
- we dissolved 0.1g of $\boldsymbol{MAT - Fe_3O_4}$in 210ml of ethanol.
- We added the previous mixture to 90ml of cooking oil.
- The mixture is placed on anUltrasonic for 30 minutes at a temperature of 65°C.
- After the reaction, the mixture is transferred to a condenser to remove the ethanol to avoid moisture, and we take the mixture to the centrifuge to remove the catalyst from it, then we added hot water twice (85 °C), each time using 25ml with stirring.
- Separation of organic (biodiesel) and aqueous phases (aqueous glycerol) for 24 hours (Figure III-8-4).

Figure III-10: The mixture (glycerol with biodiesel) in the separator for 24 hours

III-4-2-2-5-KOH as a catalyst (homogeneous basic):

During conducting experiment of production of biodiesel by the use of KOH as catalysis, next steps are followed:

- First, we dissolved 0.1g of potassium hydroxide (KOH) in 210ml of ethanol.
- We added the previous mixture to 90ml of cooking oil.
- The mixture is placed on a magnetic stirrer for 30 minutes at a temperature of 65°C.
- After the reaction, the mixture is transferred to a condenser to remove the ethanol to avoid moisture, then we added hot water twice85°C, each time using 25ml with stirring.
- Separation of organic (biodiesel) and aqueous phases (aqueous glycerol) for 24 hours (Figure III-8-4).

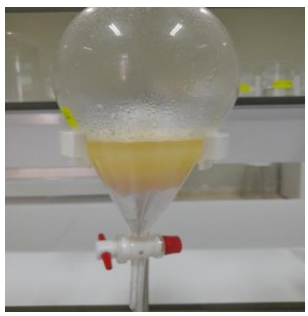

Figure III-11: The mixture (glycerol with biodiesel) in the separator for 24 hours.

III-5-Results and Discussion:

The obtained results are presented and discussed in this section

III-5-1-Calibration curve equation:

After conducting the previous experiments, absorbance of aqueous glycerol solution measured at 230 nm are listed and plotted in Table III-4 and Figure III-10, respectively.

Table III-4: Absorbance versus concentration of glycerol solutions

C (mM)	100	200	300	400	500	600	700	800	900	1000
Abs (230 nm)	0.06	0.10	0.13	0.16	0.19	0.24	0.29	0.34	0.39	0.44

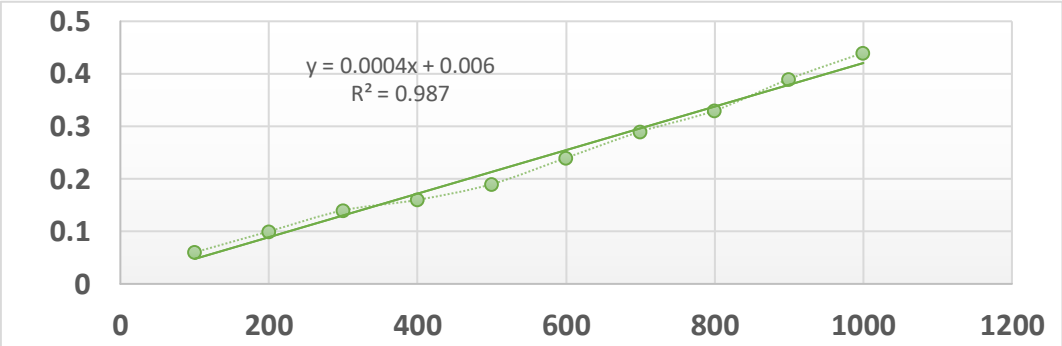

Figure III-12: calibration curve representing absorbance values as a function of glycerol concentration

From the calibration curve, it is observed that as the concentration of glycerol increases, the absorbance values also increase. Figure III-10 clearly demonstrates this relationship, showing a good linearity in the calibration curve with the equation **Y=0.0004X+0.006**and an R^2= 0.987.

III-5-2-Production of biodiesel by ethylic esterification by using different catalysts:

In all the previous experiments conducted to determine the most effective catalysts in reducing the concentration of the by-product glycerol, the following reaction mechanism was employed:

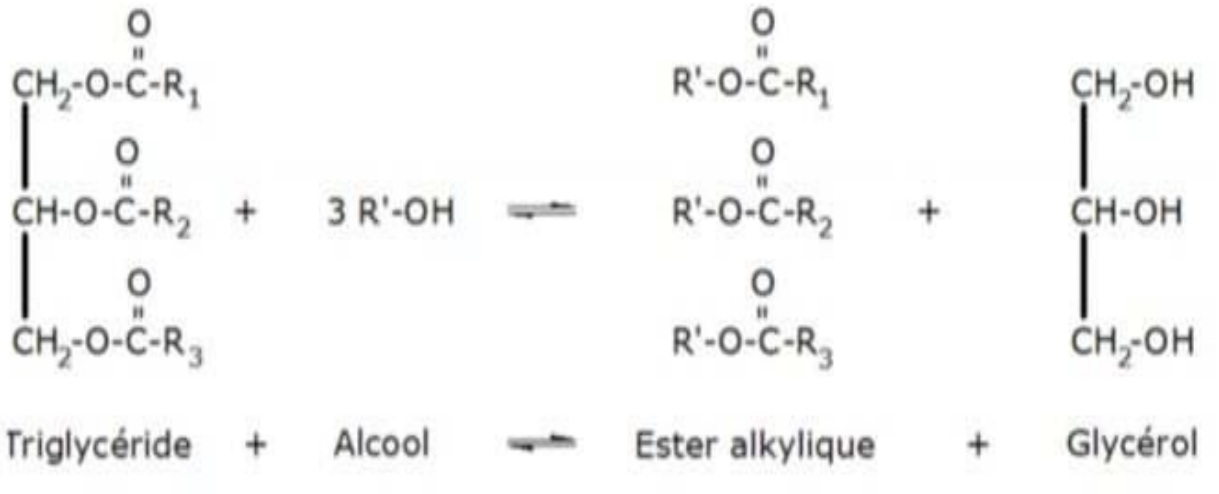

Figure III-13: The mechanism of the transesterification reaction for biodiesel production

Table III-5: measurements and results related to the produced biodiesel and glycerol

Catalyst	ARM$-Fe_3O_4$	JUN$-Fe_3O_4$	MAT $-$ Fe_3O_4	$ROS-Fe_3O_4$	KOH
Mass of biodiesel (g)	**68.99**	**66.35**	**74.13**	**68.35**	**66.5**
Density of biodiesel	**0.86**	**0.87**	**0.86**	**0.85**	**0.85**
Viscosité (40C°) (CSt)	**2.32**	**1.98**	**2.11**	**2.07**	**3.12**
Absorbance GLY	**0.242**	**0.292**	**0.141**	**0.243**	**0.291**
Biodiesel yield (%)	**81**	**85**	**91**	**84**	**82**
Concentration of produced glycerol (Mm)	**715**	**590**	**337.5**	**592.5**	**712**

After measuring the density and viscosity of the produced biodiesel, we observed that all obtained samples fell within the required range for both parameters. This indicates that all catalysts demonstrated success and effectiveness in the experiments. Based on these results, we plotted the following graphical representationwhere the yields of the produced biodiesel are presented.

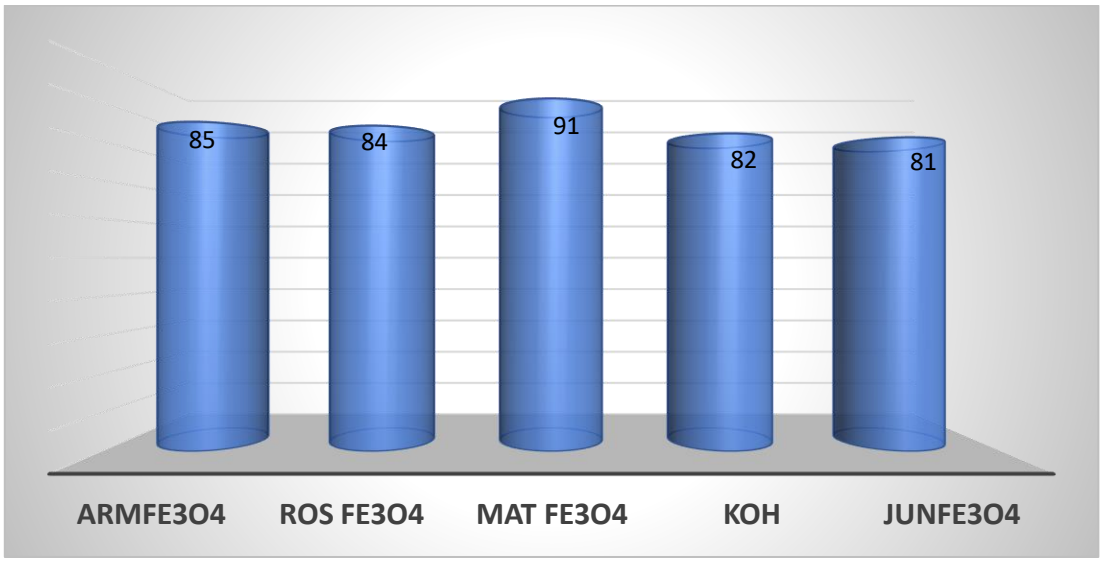

Figure III-14:biodiesel yield (%) for different catalysts

Figure III-12 shows that yields (%)of produced biodiesel by using $\boldsymbol{MAT-Fe_3O_4}$ *NPs* as catalyst is reached 91%, then $\boldsymbol{ARM-Fe_3O_4}$ 85%,next $\boldsymbol{ROS-Fe_3O_4}$84%, then KOH 82%, and finally $\boldsymbol{JUN-Fe_3O_4}$ 81%. So, the three IONPs showed highest activity in production of biodiesel compared to the basic catalyst KOH which is typically used.

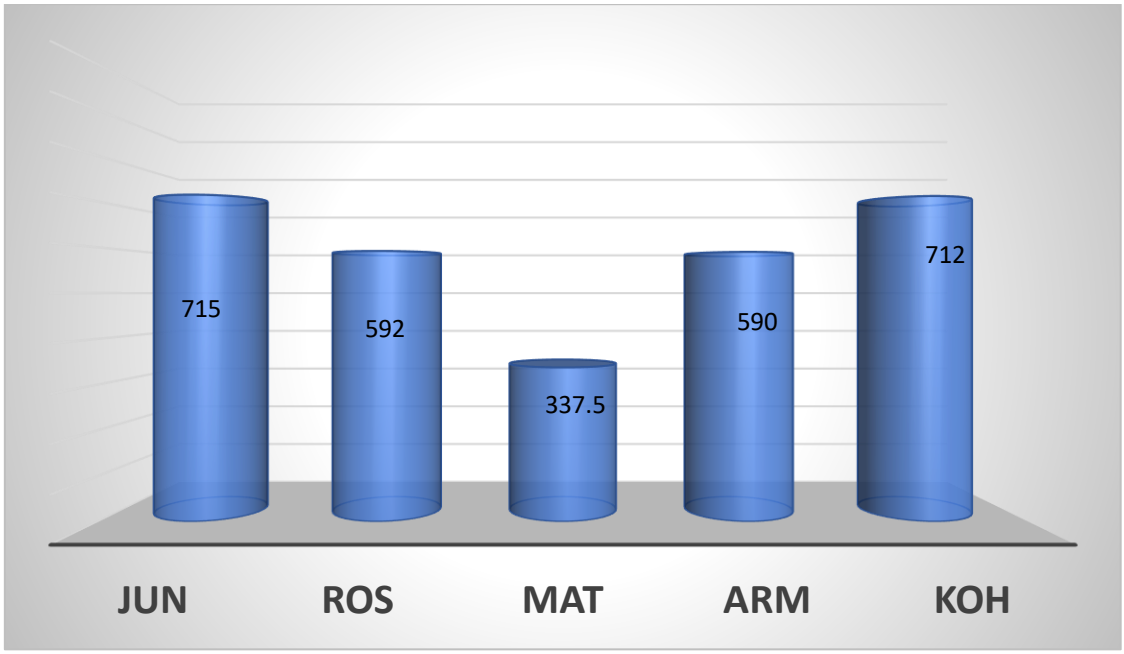

Figure III-15: concentration of produced glycerol in the five experiments

Figure III-13 shows that glycerol concentration(mM)of by-produced in production of biodiesel by using $\boldsymbol{MAT-Fe_3O_4}$ *NPs* as catalyst is reached 337.5 mM, then $\boldsymbol{ARM-Fe_3O_4}$ 590 mM,next $\boldsymbol{ROS-Fe_3O_4}$, 592 mM, then KOH ; 712 mM, and finally $\boldsymbol{JUN-Fe_3O_4}$; 715 mM.

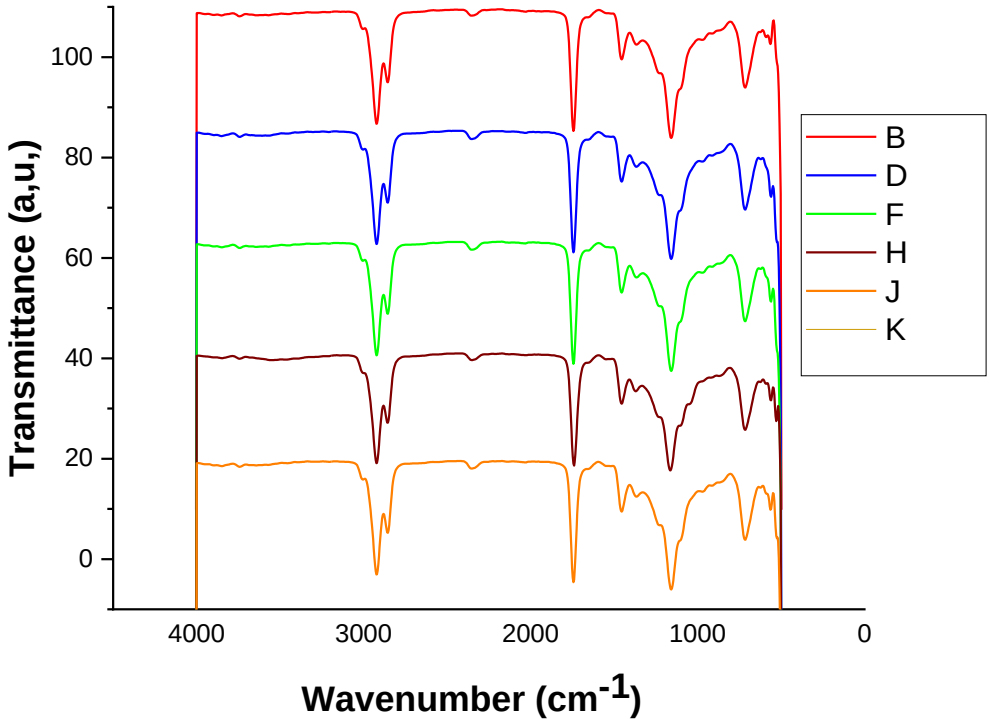

Figure III-16-The infrared IR spectrum of the biodiesel produced using various catalysts: (K)JUNFe_3O_4, (D)ARMFe_3O_4, $(B)MATFe_3O_4$, $(F)ROSFe_3O_4$, and (J)KOH

The Figure III-14shows:

- A valence vibration at 2800.75 cm^{-1}, corresponding to the C-H group of biodiesels.
- A valence vibration at 1760.82 cm^{-1}, corresponding to the ester group RCOOR and C=O stretching of biodiesel.
- A valence vibration at 1024.33 cm^{-1}, corresponding to the ester group and O stretching of biodiesel.
- A valence vibration between 3300 cm^{-1}, corresponding to the glycerol group and O-H stretching of biodiesel.

Based on the analysis of FTIR spectra presented in Figure III-14, it is easy to declare that biodiesel is formed in all cases.

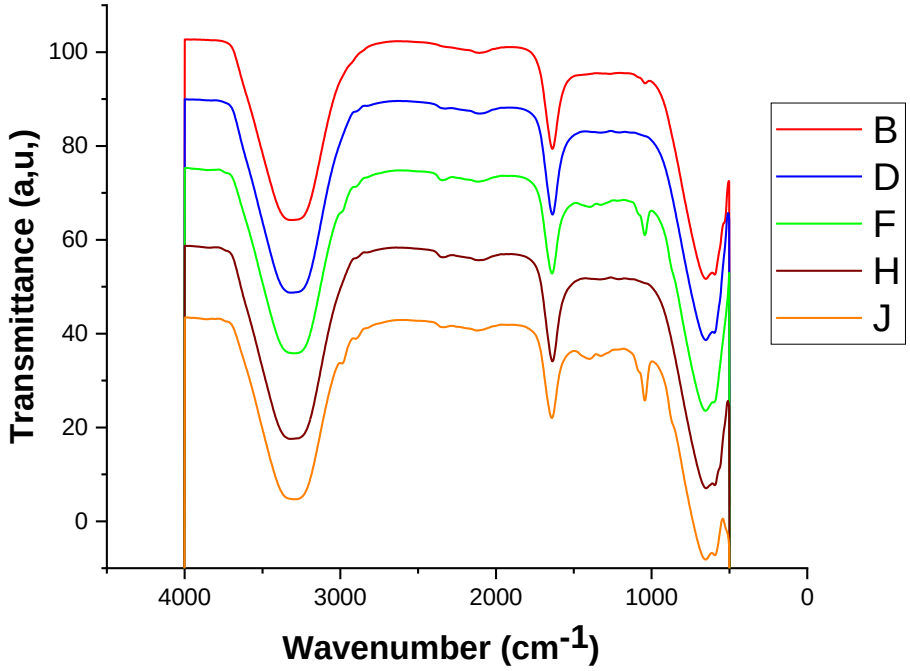

Figure III-17-The infrared IR spectrum of the glycerol produced using various catalysts: $(\boldsymbol{B})$**JUN**$\boldsymbol{Fe_3O_4}$, $(\boldsymbol{D})$**ARM**$\boldsymbol{Fe_3O_4}$, $(\boldsymbol{HMAT}\boldsymbol{Fe_3O_4}$, $(\boldsymbol{F})\boldsymbol{ROSFe_3O_4}$, $(\boldsymbol{J})$**KOH**

The Figure III-15 display that:

- Hydroxyl (OH) stretching vibration: Found typically within the range of 3200 to 3600 $\boldsymbol{cm^{-1}}$.
- Carbonyl (C=O) stretching vibration: Typically observed around 1700 $\boldsymbol{cm^{-1}}$.
- Carbonyl (C=O) bending vibration: Typically observed between 1000 and 1300 $\boldsymbol{cm^{-1}}$.
- Bonds stretching (C-C and C-H): Usually observed between 2800 and 3000 $\boldsymbol{cm^{-1}}$.

Based on the analysis of FTIR spectra presented in Figure III-15, it is easy to declare that glycerol is formed in all cases.

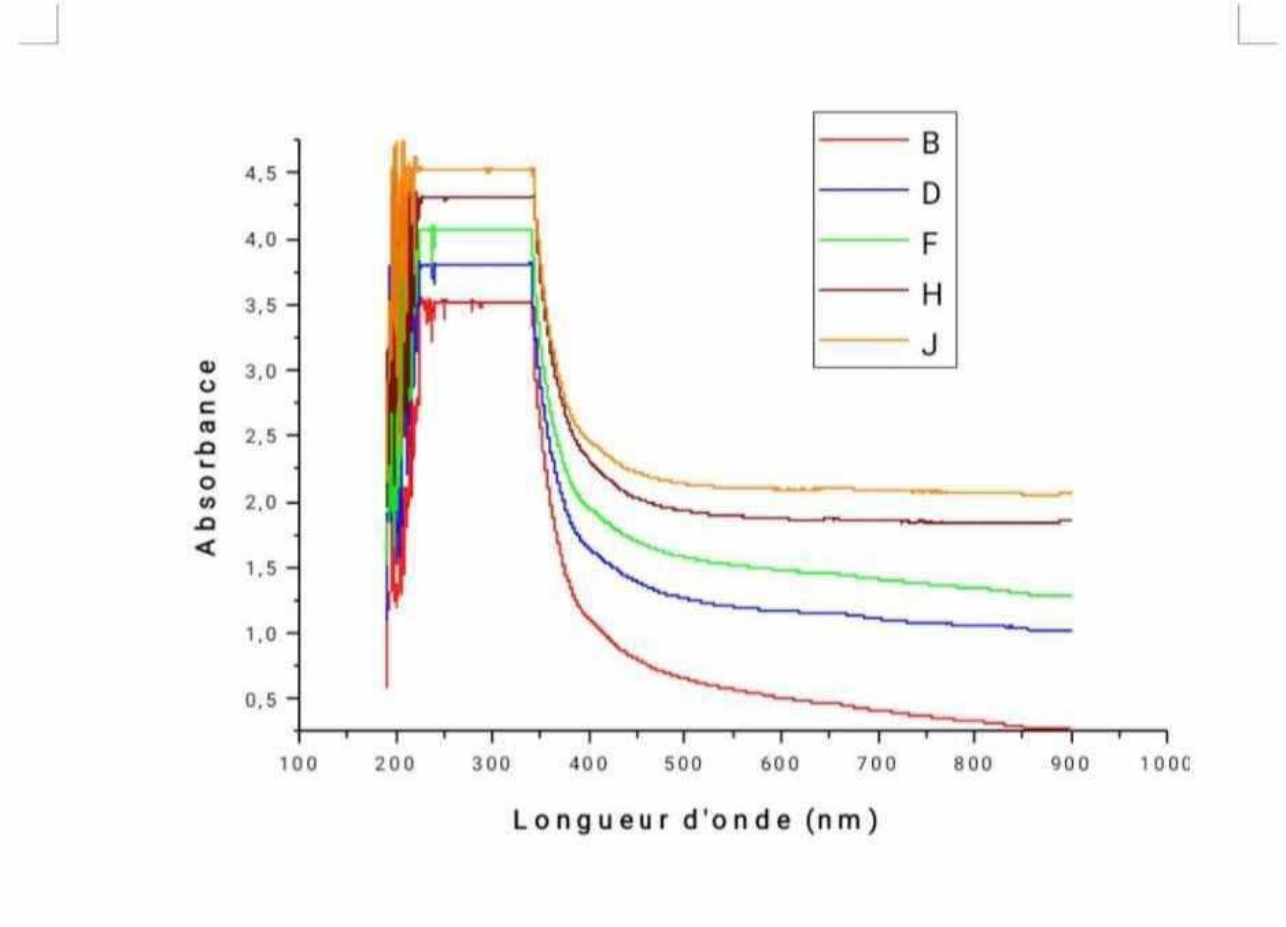

Figure III-18-The UV spectrum of the biodiesel produced using various catalysts: (B) JUN $-Fe_3O_4$, (H)ARM $-Fe_3O_4$, $(J)MAT-Fe_3O_4$, $(F)ROS-Fe_3O_4$, (D)KOH

Figure III-18 shows UV-Vis spectra of produced biodiesel. It is observed a distinct absorption peakat wavelength **350 nm**. This peakis a characteristic peak of biodiesel. The same characteristic peak is reported by [48].

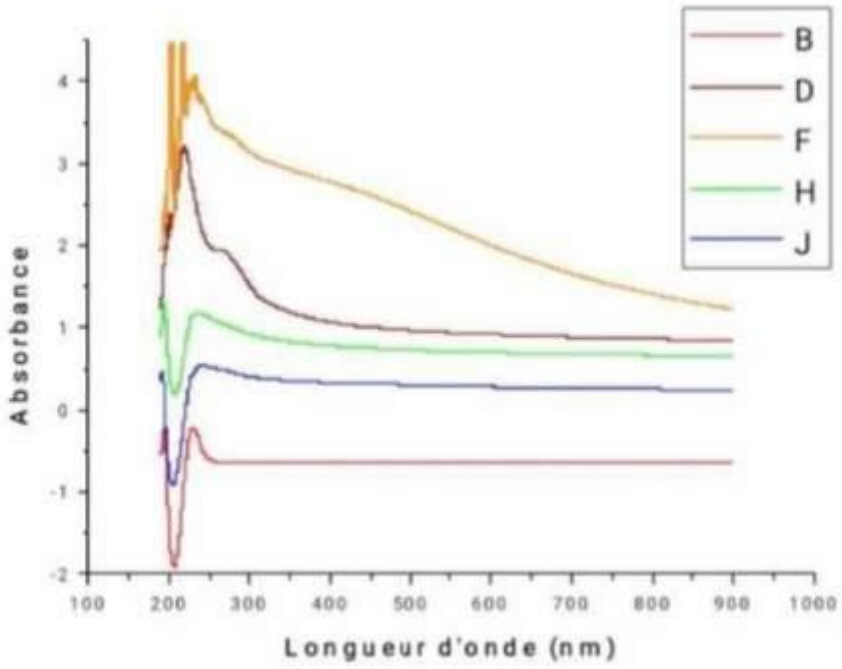

Figure III-19-The UV spectrum of the glycerol produced using various catalysts:
(B) JUN $-Fe_3O_4$, (H)ARM $-Fe_3O_4$, $(J)MAT-Fe_3O_4$, $(F)ROS-Fe_3O_4$, (D)KOH

Figure III-17 shows UV-Vis spectra of produced glycerol. It is observed a distinct absorption peakat wavelength **230 nm**. This peak is a characteristic peak of glycerol. The same characteristic peak is reported by [49].

III- 6 Conclusion:

This study focused on optimizing biodiesel production through the ethylic esterification of cooking oil using five different catalysts: ARM-Fe_3O_4, ROS-Fe_3O_4, MAT-Fe_3O_4, JUN-Fe_3O_4 nanoparticles (NPs), and KOH which is typically used. The goal was to evaluate the impact of these catalysts on the concentration of glycerol, a by-product, and the overall quality and yield of the produced biodiesel. The experiments were carried out under previously optimized conditions, including the oil/ethanol ratio, temperature, reaction time, and catalyst quantity. The findings showed that the use of ROS-Fe_3O_4, ARM-Fe_3O_4, and MAT-Fe_3O_4NPs as catalysts in biodiesel production leads to highly minimize the concentration of glycerol: 592 mM,590 Mm, and 337 mM, respectively) compared to that produced by using JUN-Fe_3O_4 NPs, and KOH which are respectively 715Mm and 712 mM. Furthermore, density (0.85 g/cm^3-0.87 g/cm^3) and kinematic viscosity (1.98CST -3.12CST) of biodiesel are found to be ininternational standards. The calculated yields of produced biodiesel are found to be 85%, 84%, 91%, 81%, and 82 % respectively to used e_3O_4, ROS-Fe_3O_4 and MAT-Fe_3O_4 NPs as catalysts in biodiesel production leads to minimize tcatalysis ARM-Fe_3O_4, ROS-Fe_3O_4, MAT-Fe_3O_4, JUN-Fe_3O_4 NPs, and KOH.

General conclusion

General Conclusion

This study explored the production of biodiesel through ethylic esterification of cooking oil using five different catalysts: ARM- Fe_3O_4, ROS- Fe_3O_4, MAT- Fe_3O_4, JUN-Fe_3O_4NPs, and KOH. The primary objective was to evaluate the impact of these catalysts on the concentration of glycerol, a by-product that can adversely affect biodiesel quality.

Experiments were carried out under previously optimized conditions, including oil/ethanol ratio, reaction temperature and time, and catalyst quantity. The results demonstrated that ROS$-Fe3O_4$, ARM-$Fe3O_4$, and MAT$-Fe_3O_4$ NPs were the most effective in minimizing glycerol concentration, achieving values of 592mM, 590 Mm, and 337mM, respectively. In contrast, the glycerol concentrations for JUN$-Fe_3O_4$ NPs, and KOH were 715 mM and 712 mM, respectively.

Additionally, the produced biodiesel met international standards for density (0.85 g/cm^3-0.87g/cm^3) and kinematic viscosity (1.98 CSt-3.12CSt). The yields of biodiesel produced were 91%, 85%, 84%, 82%,and 81% forMAT- Fe_3O_4, ARM- Fe_3O_4, ROS Fe_3O_4, KOH, and JUN- Fe_3O_4 NPs, respectively. These findings indicate that using ARM- Fe_3O_4, ROS- Fe_3O_4, and MAT Fe_3O_4-NPs as catalysts minimizes glycerol concentration and hence enhancing biodiesel yield and quality.

In conclusion, the utilization of ARM- Fe_3O_4, ROS-, Fe_3O_4 and MAT- Fe_3O_4NPs in biodiesel production processes significantly enhances the final product's quality by reducing glycerol content, thereby offering a promising approach for efficient and high-quality biodiesel production more than KOH.

The references bibliographies

The references bibliographies

[1]. http://www.eia.gov/forecasts/ieo/pdf/0484(2011).pdf.

[2]. Shay, E.G., Biomass and Bioenergy, 1993. 4(4): p. 227-242.

[3]. Srivastava, A., Prasad, R., Renewable and Sustainable Energy Reviews, 2000. 4: p.111-133

[4].www.ifp.fr/content/download/45711/1017150/version/4/file/ToutSavoirSurLesBiocarburants.pdf.

[5]. Burzynski, J.P., IFP, 2008

[6]. Spolaore, P., Joannis-Cassan, C., Duran, E., Isambert, A., Journal of Bioscience andBioengineering, 2006. 101(2): p. 87-96.

[7]. Roessler, P.G., Brown, L.M., Dunahay, T.G., Heacox, D.A., Jarvis, E.E., Schneider, J.C.,Talbot, S.G., Zeiler, K.G., Enzymatic Conversion of Biomass for Fuels Production, 1994: p.255-70.

[8]. Gavrilescua, M., Chisti, Y., Biotechnology Advances, 2005. 23: p. 471-499.

[9]. Ghirardi, M.L., Zhang, L., Lee, J.W., Flynn, T., Seibert, M., Greenbaum, E., Melis, A.,Trends in Biotechnology, 2000. 18(12): p. 506-511.

[10]. Kargı, F., Kapdan, L.K., Enz. Microb. Tech., 2006. 38(5): p. 569-582.

[11]. Chisti, M.Y., J. Ramsay Society, 1980. 27-28: p. 24-26.

[12].Nagel, N., Lemke, P., Applied Biochemistry and Biotechnology, 1990. 24-25: p. 355-361.

[13]. Gavrilescua, M., Chisti, Y., Biotechnology Advances, 2005. 23: p. 471-499.

[14]. Pinto, A.C., Guarieiro, L.L.N., Rezende, M.J.C., Ribeiro, N.M., Torres, E.A., Lopes,W.A., de P. Pereira, P.A., de Andrade, J.B., J. Braz. Chem. Soc., 2005. 16(6B): p. 1313-1330.

[15]. Stern, R., Hillion, G., Rouxel, J.J., Leporq, S., US patent 5,908,946, 1999.

[16]. Chisti, Y., Biotechnology Advances, 2007. 25: p. 294–306

[17]. Fillières, R., Université Claude Bernard-Lyon1, 1995.

[18]. Stern, R., Guibet, J.C., Graille, J., Rev. IFP, 1983. 38(1): p. 121-136.

[19]. Pinto, A.C., Guarieiro, L.L.N., Rezende, M.J.C., Ribeiro, N.M., Torres, E.A., Lopes,W.A., de P. Pereira, P.A., de Andrade, J.B., J. Braz. Chem. Soc., 2005. 16(6B): p.1313-1330.

[20]. Stern, R., Hillion, G., Rouxel, J.J., Leporq, S., US patent 5,908,946, 1999.

[21]. Chisti, Y., Biotechnology Advances, 2007. 25: p. 294–306.

[22]. PRYDE E.H., Vegetable oil standards. In: Proceedings of the International Conferenceon Plant and Vegetables Oils as Fuels, Fargo, USA, , (ASAE Publication, 4-82), p.101-105.Saint-Joseph: ASAE , (1982).

[23]. VAITILINGOM G., Huiles végétales – biocombustibles diesel : influence de lanature des huiles et en particulier de leur composition en acides gras sur la qualité-carburant,thèse de doctorat, Université d'Orléans, pp87, (1992).

[24]. SRIVASTAVA A., and PRASAD R., Triglyceride-Based diesel fuels, Renewableand Sustainable Reviews,4, 111-133 (2000).

[25]. Stansell, G . R , Gray, V.M. et Sym, S.D. (2012). Microalgal fàtty acid composition:implications for biodiesel quality. Journal o f Applied Phycology, volume 24, numéro 4,p.791-801.

[26]. Jean KOULIDIATI, Gilles VAITILINGOM. Contribution a l'étude des conditionsoptimales de combustion des huiles végétales dans les moteurs diesel et sur les brûleurs : casde l'huile de coton. (2008). PP51-55.

[27] Dobarganes C. Formation and analysis of high molecular-weight compounds in fryingfats and oils. OCL, Vol. 5, n°1, p. 41-47 (1998).

[28]. Melton SL., Jafar S., Sykes D., Tigriano MK. Review of stability measurements forfrying oils and fried food flavour. J. Am. Oil Chem. Soc., 71, p. 1301-1308 (1994).

[29]. Perkins E.G. The analysis of frying oils and fats and oils. J. Am. Oil Chem. Soc., 65,p. 520-525 (1988).

[30]. Stevenson S.G., Vaisey Genser M., Eskin N.A.M. Quality control in the use of deepfrying oils. J. Am. Oil Chem. Soc., 61, p. 1102-1108 (1984).

[31]. Sonntag, N.O.V., (4th edn. ed.),D. Swern, Editor, Bailey's Industrial Oil and FatProducts, John Wiley and Sons, New York, USA, 1979. 1: p. 99–176

[32]. Ziejewski, M., Kaufman, K.R., Pratt, G.L., Seminar II, Northern Regional ResearchCenter, Peoria, Illinois, 19-20 October, 1983.

[33]. Allinger, N.L., Cava, M. P., De Jongh, D. C., Johnson, C. R., Lebel, N. A., Stevens, C.L., 6ème ed, 1983. 2: p. 553.

[34]. H. Hazar, H. Aydin, Performance and emission evaluation of a CI engine fueled withpreheated raw rapeseed oil (RRO) - Diesel blends, Applied Energy, Vol. 87, n° 3, 2010.

[35]. A.V. Bridgwater, Renewable fuels and chemicals by thermal processing of biomass,Chemical Engineering Journal, Vol. 91, n°2, 2003.

[36].B. Hamad, Transestérification des huiles végétales par l'éthanol en conditions doucespar catalyses hétérogènes acide et basique, Thèse de doctorat, université Claude BernardLyonI, 2009

[37].B. Freedman, R.O. Butterfield, E.H. Pryde, Transesterification kinetics of Soybean oil1,Journal of the American Oil Chemists' Society, Vol. 63, n° 10, 1986.

[38]. M.K. Lam, K.T. Lee, A.R. Mohamed, Homogeneous, heterogeneous and enzymaticcatalysis for transesterification of high free fatty acid oil (waste cooking oil) to biodiesel: Areview, Biotechnology advances, Vol. 28, n° 4, 2010.

[39]. La production de biodiesel à partir de cultures oléagineuses, Publication no EVC 031

[40].ScienceDaily, Phys.org,Nanowerk .

[41].Journal of CatalysisElectrochimicaActa .

[42].Nanomaterials Science: An Introduction, Introduction to Nanoscience and Nanotechnology"

[43].United Nations Environment Programme,European Environment Agency .

[44].PubMed ,ScienceDirect .

[45]. The International Renewable Energy Agency (IRENA) and the International Energy Agency (IEA).

[46]. Chemical Engineering Journal," "Catalysis Today," "Applied Catalysis A: General"

[47]. Plant extract FRAP effect on cation vacancies formation in greenly synthesized wüstite (FexO) nanoparticles: A new contribution

.[48]. Spectroscopy analysis of hetrogeneous Biocatalysts for biodiesel production from expired sunflower cooking oil.

[49]